Journal of Neuropathology and Experimental Neurology

Vol. 61, No. 11
November, 2002
pp. 984–991

Promyelocytic Leukemia Protein Is Redistributed during the Formation of Intranuclear Inclusions Independent of Polyglutamine Expansion: An Immunohistochemical Study on Marinesco Bodies

SATOKO KUMADA, MD, PHD, TOSHIKI UCHIHARA, MD, PHD, MASAHARU HAYASHI, MD, PHD, AYAKO NAKAMURA, ETSUKO KIKUCHI, TOSHIO MIZUTANI, MD, PHD, AND MASAYA ODA, MD, PHD

Abstract. Marinesco bodies (MBs) are ubiquitinated intranuclear inclusions observed in nigral pigmented neurons. They increase in number during aging, and their formation is considered to represent a cellular reaction to stress, but is not always associated with neuronal degeneration. We conducted immunohistochemical studies on MBs abundant in myotonic dystrophy brains and compared their nature with that of neuronal intranuclear inclusions (NIIs) in polyglutamine diseases. First, we examined the relationship between MBs and polyglutamine proteins and demonstrated that one of the polyglutamine proteins, ataxin-3, as well as a 19S proteasomal protein, was preferentially recruited into MBs even in the absence of expanded polyglutamine. This indicates that an alternative mechanism during the formation of MBs that is not related to polyglutamine expansion or neuronal degeneration may recruit ataxin-3 into nuclear inclusions in a protein-specific manner. Secondly, we investigated the relationship between MBs and promyelocytic leukemia protein (PML), a nuclear matrix-associated protein that is normally localized to intranuclear punctate structures (PML nuclear bodies) and is known to reorganize itself in association with polyglutamine aggregation. In nigral pigmented neurons in myotonic dystrophy, spherical, hemispherical or rod-like PML-immunoreactive structures, in addition to punctate structures, were observed in their nuclei. Similar PML redistribution was also observed in nigral pigmented neurons in aged controls and cases of hepatic encephalopathy, 2 other conditions in which abundant MBs are formed. Double immunofluorescence study revealed that these PML-positive structures undergo morphological changes in association with ubiquitin accumulation during MB formation. It is therefore indicated that PML reorganization does not represent a specific nuclear event involved in the pathogenesis of polyglutamine diseases, but may commonly occur during the formation of intranuclear inclusions as a reaction against various stresses that involve the ubiquitin-proteasome pathway.

Key Words: Ataxin-3; Hepatic encephalopathy; Marinesco body; Myotonic dystrophy; Neuronal intranuclear inclusions; Polyglutamine; Promyelocytic leukemia protein.

INTRODUCTION

A cytopathological hallmark of polyglutamine diseases is the presence of neuronal intranuclear inclusions (NIIs) harboring disease-related proteins containing abnormally expanded polyglutamines (1). Since the artificial overexpression of truncated proteins containing expanded polyglutamines in some cellular or animal models results in the formation of intranuclear aggregates and causes cell death (2–6), it has been speculated that the NII formation plays a key role in the pathogenesis of polyglutamine diseases. Recently, several studies indicated that a nuclear matrix-associated protein, promyelocytic leukemia protein (PML), is redistributed during the formation of NIIs (2, 7–10). PML is a major component of nuclear subdomains, namely PML nuclear bodies, which appear normally as punctate structures scattered in the nuclei (11). In cells transfected with mutant ataxin-1 (2) or mutant ataxin-3 (7), PML altered its normal distribution and was colocalized to nuclear aggregates formed by mutant proteins. A similar reorganization of PML nuclear bodies around NIIs was also observed in human brains with dentatorubral-pallidoluysian atrophy (DRPLA), Machado-Joseph disease (MJD)/spinocerebellar ataxia type 3 (SCA3) (8, 9), and SCA7 (10). Because PML mediates multiple apoptotic pathways (12, 13) and the disruption of PML nuclear bodies plays a fundamental role in the oncogenic mechanism of acute promyelocytic leukemia (14), it was speculated that a critical step in polyglutamine pathogenesis also involves the alternation of this subnuclear domain (2, 9, 15). One of the questions to be addressed is, therefore, how PML is involved in the formation of NIIs and neurodegeneration.

In this study, we focused on another example of ubiquitinated intranuclear inclusions in the pigmented neurons of the substantia nigra, Marinesco bodies (MBs), which are formed abundantly in the absence of expanded polyglutamine. Because their abundance in several conditions (e.g. aging [16, 17], hepatic encephalopathy [18], or myotonic dystrophy [19]) is not necessarily associated with degenerative changes in the nigral pigmented neurons (18), this study provides us with an opportunity to observe the formation process of nuclear inclusions not related to polyglutamine expansion or cell degeneration. We previously reported that MBs of aged controls and those of patients with hepatic encephalopathy contain

From the Department of Pediatrics (SK), Metropolitan Fuchu Medical Center for Severe Motor and Intellectual Disabilities, Tokyo, Japan; Department of Neuropathology (TU, AN) and Department of Clinical Neuropathology (MH, EK), Tokyo Metropolitan Institute for Neuroscience, Tokyo, Japan; Department of Pathology (TM, MO), Tokyo Metropolitan Neurological Hospital, Tokyo, Japan.

Correspondence to: Dr. Satoko Kumada, Department of Pediatrics, Metropolitan Fuchu Medical Center for Severe Motor and Intellectual Disabilities, 2-9-2, Musashidai, Fuchu-shi, Tokyo, 183-0042, Japan.

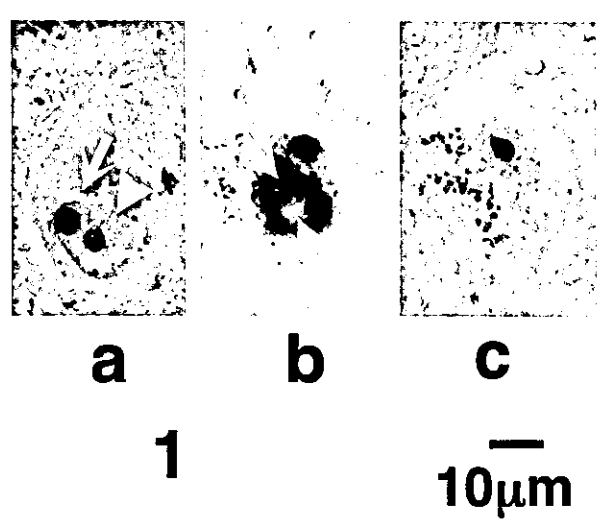

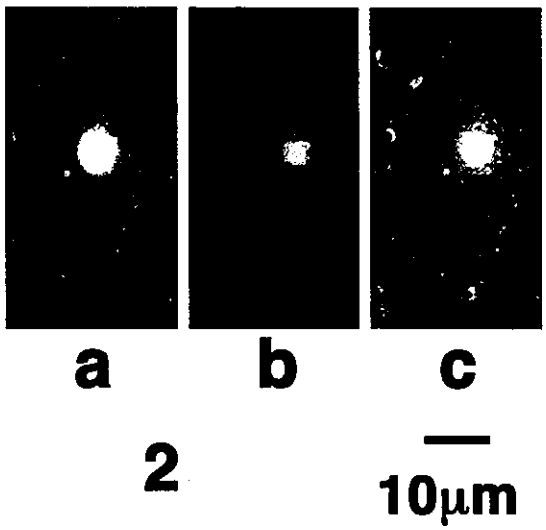

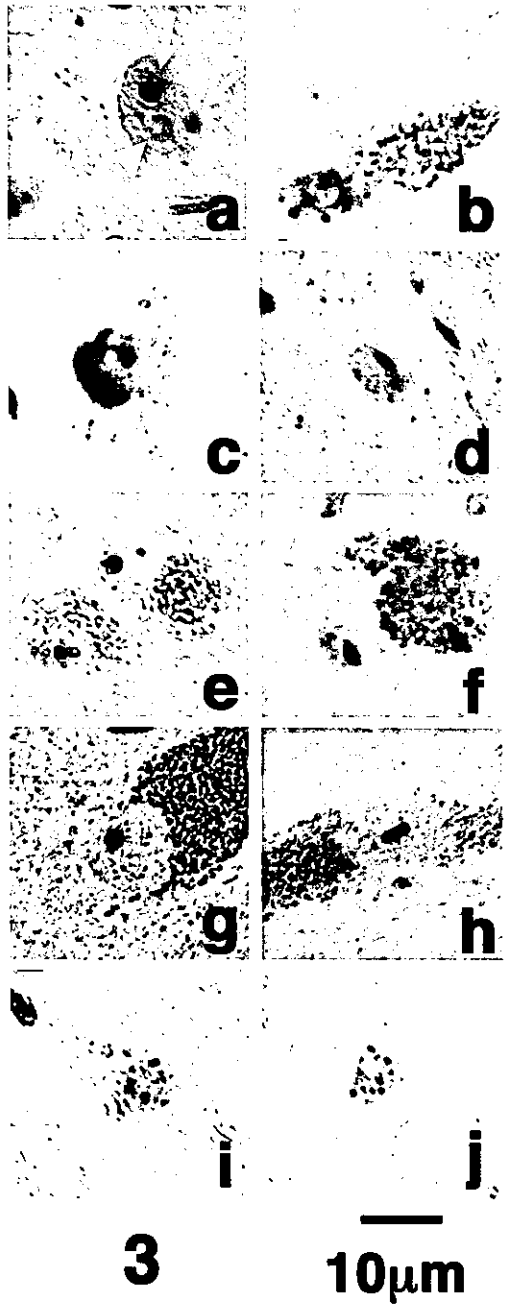

Fig. 1. Immunohistochemical studies of nigral pigmented neurons in myotonic dystrophy. a: MBs were immunopositive for anti-ubiquitin antibody (arrow), which were distinct from nucleoli counterstained by hematoxylin (arrowhead). b: Double immunohistochemical staining with antibodies against ataxin-2 and ubiquitin revealed that ataxin-2 was immunoreactive in the nucleoplasm, but not in the nucleoli (arrowhead) or MBs (arrows). c: Ataxin-3 immunolabeling was manifested as intranuclear inclusions.

Fig. 2. Double immunofluorescence staining of MB in myotonic dystrophy. a: Ubiquitin immunoreactivity. b: Ataxin-3 immunoreactivity. c: Merged image of (a) and (b). Ataxin-3 is localized in the core of MBs, surrounded by ubiquitin. These images of the same neuron were obtained by confocal microscopy.

Fig. 3. Immunohistochemical studies of nigral pigmented neurons in myotonic dystrophy (a–d). a: Immunoreactivity of MSS1, a subunit of ATPase of 19S proteasome, was manifested as intranuclear inclusions (arrows), distinct from nucleoli (arrowhead). b: PML labeling was present in nuclei as a granular pattern in about half of the nigral pigmented neurons. However, other neurons showed larger sized spherical (c) or rod-like (d) PML-immunoreactive structures. Immunohistochemical studies of nigral pigmented neurons in cases of hepatic encephalopathy (e and f) and aged controls (g and h). Spherical (e and g) or rod-like (f and h) PML-positive structures were observed in both conditions. Immunohistochemical studies of thalamic neurons (i) and Purkinje cells (j) in myotonic dystrophy. PML-like immunoreactivity appeared only as a fine granular pattern.

TABLE
Proportion of Nigral Pigmented Neurons Harboring Marinesco Bodies (MBs)*

Case	Age/sex	Disease	% of MBs
Myotonic dystrophy cases			
1	35/F	Myotonic dystrophy	18.8
2	46/F	Myotonic dystrophy	39.5
3	52/F	Myotonic dystrophy	15.4
4	54/M	Myotonic dystrophy	17.1
5	57/M	Myotonic dystrophy	22.5
6	59/M	Myotonic dystrophy	29.3
7	65/F	Myotonic dystrophy	32.4
Hepatic encephalopathy cases			
8	55/M	Hepatic encephalopathy	16.7
9	58/F	Hepatic encephalopathy	43.1
10	79/M	Hepatic encephalopathy	32.1
Aged controls			
11	52/M	Lung cancer	20.6
12	55/M	Leukemia	16.7
13	63/M	Thyroid cancer	18
14	70/M	Bladder cancer	29.5
15	76/F	Malignant lymphoma	25.6
Young controls			
16	22/M	Sepsis	0
17	29/F	Guillain-Barré syndrome	0

* The percentage (%) of MBs is the percentage of nigral pigmented neurons harboring MBs.

a polyglutamine protein, ataxin-3, in the absence of expanded polyglutamine (20, 21). As ubiquitin and ataxin-3 are commonly recruited into NIIs of polyglutamine diseases (22), MBs share the immunohistochemical characteristics of NIIs seen in polyglutamine diseases. In this study, these immunohistochemical characteristics of MBs were confirmed in cases of myotonic dystrophy. In addition, we demonstrated for the first time that the reorganization of PML nuclear bodies occurs during MB formation, independent of polyglutamine expansion.

MATERIALS AND METHODS

Immunohistochemical Examination of Nigral Pigmented Neurons in Myotonic Dystrophy

The clinical subjects comprised 7 cases of myotonic dystrophy (Table). The diagnosis was made on the basis of characteristic clinical features, such as frontal baldness, cataracts, cardiac conduction abnormalities, testicular atrophy, and endocrine abnormalities, in addition to the presence of clinical and electrical myotonia and distal-dominant myopathy (23). Each case showed the neuropathological features of myotonic dystrophy, including abundant thalamic inclusions (19), neurofibrillary tangles unaccompanied by senile plaques in the parahippocampal gyrus (24), and myelin loss of the white matter in the anterior temporal lobes (25, 26), as confirmed by TM, MO, SK, and MH.

The examination of patient tissues was conducted after written consent was provided by the next of kin and with the approval of the institutional committee. Formalin-fixed paraffin-embedded blocks of the midbrain were examined. Four-μm-thick sections were immunohistochemically stained by standard avidin-biotin-peroxidase complex (ABC) methods. The following antibodies were used: anti-ubiquitin (dilution 1:10,000, mouse monoclonal, Chemicon, Temecula, CA), anti-polyglutamine 1C2 (dilution 1:10,000, mouse monoclonal, Chemicon), anti-ataxin-2 15F6 (dilution 1:100, mouse monoclonal, IgM class, Imochem, Christchurch, New Zealand), anti-ataxin-3 A3C–1 (dilution 1:1,000, rabbit polyclonal) (20), anti-PML (dilution 1:3,000, rabbit polyclonal, MBL, Nagoya, Japan) (27), and anti-ATPase subunit MSS1 of 19S proteasome (dilution 1:10,000, rabbit polyclonal, Affiniti, Exeter, UK). To expose the antigenic epitopes, sections were treated as follows: immersed in 99% formic acid for 5 min for anti-ubiquitin, autoclaved in 10 mM citrate buffer (PH 6.0) for 20 min for 1C2, 15F6, anti-PML, and anti-MSS1, or irradiated in a microwave oven for 5 min × 3 times in 0.01 M citrate buffer (PH 6.0) for A3C–1. The sections were incubated with one of the primary antibodies for 48 hours (h) at 4°C. After incubation with an appropriate biotinylated secondary antibody, color was developed using ABC (ABC Elite, Vector, Burlingame, CA) with diaminobenzidine as the chromogen. If necessary, nickel ammonium chloride was added to enhance immunolabeling (28).

The relationship between the ubiquitin epitope and either the ataxin-3 or PML epitope was examined by double immunofluorescence labeling. After being autoclaved in the citrate buffer as above, sections were incubated for 48 h with a mixture of anti-ubiquitin (1:10,000) and either A3C–1 (1:50) or anti-PML (1:300) antibodies. These sections were then incubated for 2 h with a mixture of anti-mouse IgG antibody coupled with Rhodamine red (1:200, emission peak 590 nm, Jackson Immuno Research, West Grove, PA) and anti-rabbit IgG antibody coupled with FITC (1:200, emission peak 518 nm, Cappel, Durham, NC). Other sections were incubated with a mixture of anti-mouse IgG antibody coupled with FITC (1:200, emission peak 518 nm, Cappel) and anti-rabbit IgG antibody coupled with Texas red (1:200, emission peak 596 nm, ICN, Aurora, Ohio) for comparison, giving essentially the same results. Confocal images were obtained through a Leica TCS-SP laser confocal microscope (Heidelberg, Germany).

Immunohistochemical Examination of the Extranigral Regions in Myotonic Dystrophy and the Substantia Nigra in Hepatic Encephalopathy, Aged and Young Controls

Sections of the thalamus, cerebellum, temporal lobe including hippocampus, and spinal cord were examined in all 7 cases of myotonic dystrophy. In addition, sections of the midbrain were examined in 3 cases of hepatic encephalopathy, 5 aged controls, and 2 young controls. The latter two showed no morphological abnormalities in the central nervous system (Table).

Measurement of the PML-Positive and/or Ubiquitin-Positive Intranuclear Structures

The areas of the PML-positive and/or ubiquitin-positive intranuclear structures were measured in 62 and 70 nigral pigmented neurons in the cases of myotonic dystrophy and young

controls, respectively, on confocal images at the optical plane showing the maximum cross-sectional areas, using the NIH image.

RESULTS

In all the cases examined there was neither apparent neuronal loss nor gliosis in the substantia nigra. MBs, ubiquitin-positive intranuclear inclusions (Fig. 1a), were abundantly observed in nigral pigmented neurons in the cases of myotonic dystrophy, hepatic encephalopathy, and aged controls, but not in the young controls (Table). Immunohistochemical studies for polyglutamine proteins were conducted on nigral pigmented neurons in myotonic dystrophy. Immunoreactivity for 1C2 was not detected in the nuclei. Immunoreactivity for ataxin-2, the protein encoded by the SCA2 gene, was observed in the nucleoplasm of pigmented neurons, but not nucleoli or MBs (Fig. 1b). In contrast, MBs were immunopositive for ataxin-3, the protein encoded by the MJD/SCA3 gene (Fig. 1c), and the double immunofluorescence study demonstrated that ataxin-3 and ubiquitin epitopes were colocalized in the inclusions, with the former always accumulating in the center, surrounded by the latter (Fig. 2a–c).

MBs were immunopositive for MSS1, a subunit of ATPase of 19S proteasome, which is involved in the ubiquitin-proteasome pathway for protein degradation (Fig. 3a). In about half of the nigral pigmented neurons in myotonic dystrophy, PML-like immunoreactivity was seen as intranuclear fine granules, as described in the literature (PML nuclear bodies) (11) (Fig. 3b). However, in other pigmented neurons, PML-like immunoreactivity was seen as larger-sized spherical, hemispherical, or rod-like structures (Fig. 3c, d). Similar PML redistribution was also observed in nigral pigmented neurons in cases of hepatic encephalopathy (Fig. 3e, f) and aged controls (Fig. 3g, h), in which abundant MBs were seen. In contrast, in neurons in the thalamus, cerebellum, temporal lobe, and spinal cord in myotonic dystrophy, where no intranuclear inclusions were observed, PML-like immunoreactivity was present only as a finely granular pattern (Fig. 3i, j). The double immunofluorescence study with anti-ubiquitin and anti-PML antibodies was conducted in the young controls and cases of myotonic dystrophy to examine the relationship between MBs and PML. In nigral pigmented neurons in the young controls in which no MBs were seen, 5 to 10 PML-positive fine granules were observed in the nuclei, whereas no ubiquitin-positive structures were demonstrated (Fig. 4a). On the other hand, in myotonic dystrophy, several kinds of PML and/or ubiquitin positive intranuclear structures were seen in nigral pigmented neurons. They were classified as follows: group 1, several PML-positive fine granules not colocalized to ubiquitin epitope, which were similar to those observed in the young controls (Fig. 4b); group 2, larger PML-positive spherical or hemispherical structures containing the ubiquitin epitope (Fig. 4c), coexisting with a few PML-positive fine granules; group 3, hemispherical, spherical, or rod-like PML-positive structures containing the ubiquitin epitope, which were adjacent to much larger ubiquitin-positive spheres (Fig. 4d, e); group 4, large ubiquitin-positive spheres. These spheres were flanked by PML-positive microparticles that were smaller than the PML-positive granules observed in group 1 (Fig. 4f). The PML-positive granules seen in group 1 were rarely observed in the neurons of groups 3 and 4. The PML redistribution shown in groups 2 to 4 was always associated with ubiquitin accumulation. We measured the areas of the PML- and/or ubiquitin-positive structures on confocal images showing the maximum cross-sectional areas. In myotonic dystrophy, the larger areas occupied by either PML-positive or ubiquitin-positive structures were compared among each group. They were smallest in group 1, medium-sized in group 2, and largest in groups 3 and 4 (Fig. 5a). Non-parametric analysis using the Kruskal-Wallis test revealed that their size difference among the 3 groups was statistically significant ($p < 0.0001$). We also measured the areas of the PML-positive granules in the young controls (Fig. 5b) and they were as small as those in group 1 myotonic dystrophy, verified by non-parametric analysis using the Mann-Whitney *U*-test.

DISCUSSION

MBs are the eosinophilic intranuclear inclusions observed in pigmented neurons in the substantia nigra. Although their pathogenesis remains to be elucidated, it is speculated that their formation may represent a cellular reaction to a certain kind of stress, because they increase in number during aging (16, 17) and under pathological conditions related to metabolic errors, such as hepatic encephalopathy (18). This hypothesis is further supported by the fact that MBs contain ubiquitin (29), which plays a crucial role in the removal of damaged proteins (30). We have previously demonstrated that one of the polyglutamine proteins, ataxin-3, is recruited into MBs in the brains of aged people and patients with hepatic encephalopathy (20, 21). In this study, the recruitment of ataxin-3 into MBs was also confirmed in myotonic dystrophy, another condition known to show numerous MBs (19). These observations indicate that ataxin-3 is a common component of MBs, regardless of their pathological origin. In polyglutamine diseases, wild-type polyglutamine proteins are recruited into NIIs formed in the presence of pathologically-expanded polyglutamine, which leads to the hypothesis that an interaction between expanded and non-expanded polyglutamines is a prerequisite for the nuclear translocation of wild-type polyglutamine proteins (22, 31). In our studies, however, wild-type ataxin-3 was

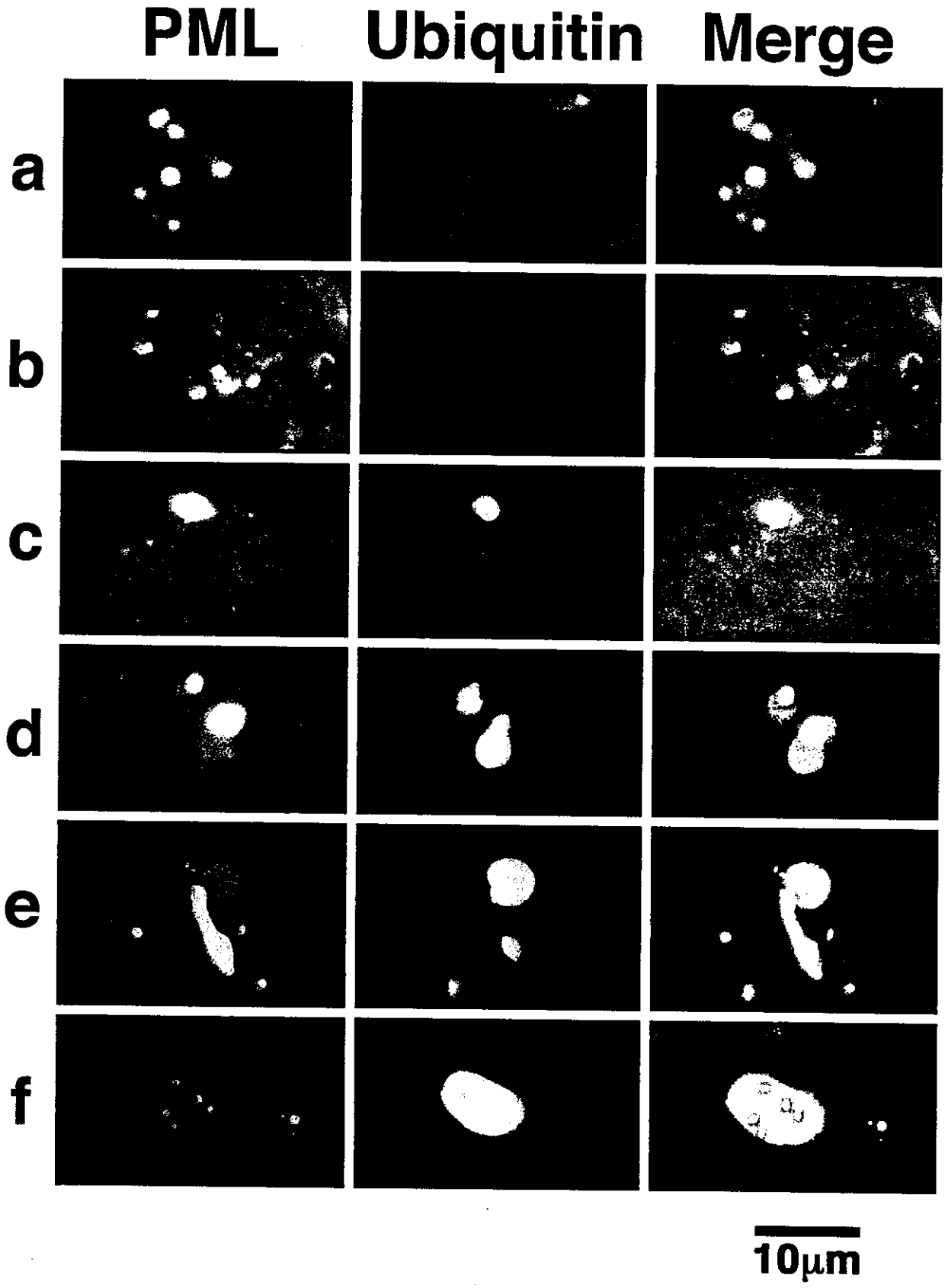

Fig. 4. Double immunofluorescence stainings with anti-PML and anti-ubiquitin antibodies of nigral pigmented neurons in young controls (a) and myotonic dystrophy (b–f). a: In the young controls, 5 to 10 PML-positive fine granules were observed in the nuclei, whereas no ubiquitin-positive structures were demonstrated. In myotonic dystrophy, several kinds of PML- and/or

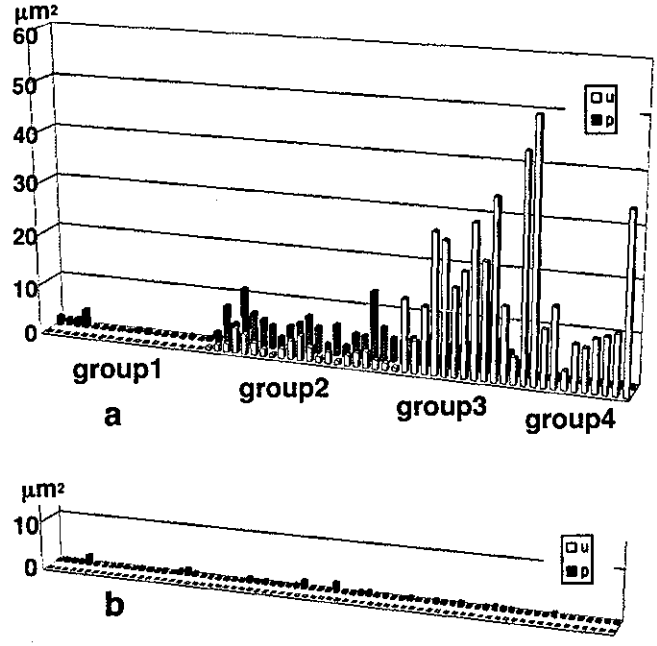

Fig. 5. The areas of the ubiquitin- and/or PML-positive intranuclear structures in 62 neurons in myotonic dystrophy (a) and in 70 neurons in young controls (b). These were measured on the confocal images of double immunofluorescence staining. u = areas of ubiquitin-positive structures; p = areas of PML-positive structures.

recruited into MBs in the absence of expanded polyglutamine. It is therefore suggested that ataxin-3 may be recruited into nuclear inclusions in a protein-specific manner, independent of polyglutamine-polyglutamine interaction. Interestingly, ataxin-3 was always concentrated in the center of MBs surrounded by the ubiquitin epitope in myotonic dystrophy, as shown in aged controls and cases of hepatic encephalopathy (20, 21). Furthermore, this characteristic morphological feature is also shared with NIIs of MJD/SCA3 brains (20). Although the physiological and pathological roles of ataxin-3 have not yet been clarified, these observations suggest that ataxin-3, like ubiquitin, may be involved in cellular reactions to stress, and is commonly recruited into intranuclear inclusions even before ubiquitin accumulation.

Another intriguing feature revealed by this study is the morphological changes of PML nuclear bodies in nigral pigmented neurons. These alternations were commonly observed in myotonic dystrophy, hepatic encephalopathy (Fig. 3e, f), and aging (Fig. 3g, h), in which abundant MBs were formed, while they were not demonstrated in the young controls in whom MBs were absent. Furthermore, this alteration of PML was not found in the extranigral areas (thalamus, cerebellum, temporal lobe, and spinal cord) in myotonic dystrophy brains. It is therefore likely that the morphological changes of PML nuclear bodies are not specific to myotonic dystrophy, but are linked to the formation of MBs in general, regardless of their underlying condition. The double immunofluorescence study revealed that some PML-containing structures were intermingled with ubiquitin-positive structures, which probably represent the intermediate phases of MB formation. Our morphometric approach further clarified that progressive ubiquitin accumulation was associated with a gradual increase in the size of these structures. These observations suggest the following hypothesis for the process of MB formation: Ubiquitin, which initially accumulates within PML nuclear bodies (group 2), may undergo subsequent modification through progressive enlargement (group 3), finally leading to the formation of large intranuclear structures, MBs, in which PML nuclear bodies are disrupted (group 4).

Although the association of PML with intranuclear aggregates has been described in DRPLA, MJD/SCA3 (8, 9), and SCA7 (10) brains, this is the first study that demonstrated how ubiquitin and PML interrelate during the formation of intranuclear inclusions in human brains. More importantly, our study demonstrated that PML involvement in the formation of intranuclear inclusions was not restricted to the pathological processes triggered by polyglutamine expansion, but was also shared with other pathological states. The function of PML nuclear bodies is not fully understood. Since they are involved in apoptosis (12, 13), it has been hypothesized that their alternation may be closely linked to neuronal degeneration in polyglutamine diseases (2, 15). However, because MB formation is not always associated with neuronal depletion, as shown in this study, the reorganization of PML nuclear bodies is not necessarily linked to neuronal death. It was recently demonstrated that mutated forms of the influenza virus nucleoprotein, which are misfolded and are therefore usually rapidly degraded by proteasomes, accumulated within PML nuclear bodies when proteasomes were inhibited. Their accumulation in PML nuclear bodies was followed by the recruitment of proteasomes and molecular chaperones (32). It is therefore suggested that PML nuclear bodies serve as an intranuclear center for the ubiquitin-proteasomal degradation, where misfolded proteins are accumulated (32). Interestingly, recent

←

ubiquitin-positive intranuclear structures were seen. b: PML-positive fine granules in the absence of ubiquitin-positive structures. c: Larger PML-positive hemispherical structure containing the ubiquitin epitope. Spherical (d) or rod-like (e) PML-positive structures containing the ubiquitin epitope, which were adjacent to much larger ubiquitin-positive spheres. f: Large ubiquitin-positive spheres, flanked by PML-positive microparticles.

studies on SCA1 (33) and MJD/SCA3 (7) have revealed that proteasomes and molecular chaperones were also recruited into nuclear aggregates of mutant proteins formed in association with PML, both in human brains and in transfected cells. In our study also, one of the proteasomal proteins, MSS1, was recruited into MBs. In addition, the PML redistribution in nigral pigmented neurons was always associated with ubiquitin accumulation, and neither occurred individually. It is therefore suggested that activation of the ubiqutin-proteasomal pathway to degrade misfolded proteins (similar to that observed in viral experiments) occurs in both the nuclear aggregates of polyglutamine diseases and MBs. These observations indicate that the reorganization of PML nuclear bodies does not represent a specific nuclear event in the neurodegeneration of polyglutamine diseases, but may occur as a common cellular reaction against an overload of misfolded proteins, triggered by either viral infection, polyglutamine expansion, or cellular stress.

In summary, in this study of MBs we have clarified that at least 2 cellular events, the translocation of ataxin-3 into the nucleus and the redistribution of PML nuclear bodies (which have previously been considered to be specifically related to polyglutamine pathology) can occur independently of polyglutamine expansion. These events may rather occur as a cellular reaction against various stresses, which finally leads to the formation of intranuclear inclusions, such as MBs. Furthermore, the occurrence of these events in neurons without any evidence of degeneration, as shown in our study, indicates that cell death is not a necessary accompaniment to the formation of nuclear inclusions. Further investigations into the pathomechanism of MBs and their possible relation to cell death may be useful to elucidate the pathological relevance of intranuclear inclusions in various disorders, including polyglutamine diseases.

REFERENCES

1. Ross CA. Intranuclear neuronal inclusions: A common pathogenic mechanism for glutamine-repeat neurodegenerative diseases? Neuron 1997;19:1147–50
2. Skinner PJ, Koshy BT, Cummings CJ, et al. Ataxin-1 with an expanded glutamine tract alters nuclear matrix-associated structures. Nature 1997;389:971–74
3. Igarashi S, Koide R, Shimohata T, et al. Suppression of aggregate formation and apoptosis by transglutaminase inhibitions in cells expressing truncated DRPLA protein with an expanded polyglutamine stretch. Nature Genet 1998;18:111–17
4. Paulson HL, Perez MK, Trottier Y, et al. Intranuclear inclusions of expanded polyglutamine protein in spinocerebellar ataxia type 3. Neuron 1997;19:333–44
5. Ikeda H, Yamaguchi M, Sugai S, Aze Y, Narumiya S, Kakizuka A. Expanded polyglutamine in the Machado-Joseph disease protein induces cell death in vitro and in vivo. Nature Genet 1996; 13:196–202
6. Martindale D, Hackam A, Wieczorek A, et al. Length of huntingtin and its polyglutamine tract influences localization and frequency of intracellular aggregates. Nature Genet 1998;18:150–54
7. Chai Y, Koppenhafer SL, Shoesmith SJ, Perez MK, Paulson HL. Evidence for proteasome involvement in polyglutamine disease: Localization to nuclear inclusions in SCA3/MJD and suppression of polyglutamine aggregation in vitro. Hum Mol Genet 1999;8: 673–82
8. Yamada M, Wood JD, Shimohata T, et al. Widespread occurrence of intranuclear atrophin-1 accumulation in the central nervous system neurons of patients with dentatorubral-pallidoluysian atrophy. Ann Neurol 2001;49:14–23
9. Yamada M, Sato T, Shimohata T, et al. Interaction between neuronal intranuclear inclusions and promyelocytic leukemia protein nuclear and coiled bodies in CAG repeat diseases. Am J Pathol 2001;159: 1785–95
10. Takahashi J, Fujigasaki H, Zander C, et al. Two populations of neuronal intranuclear inclusions in SCA7 differ in size and promyelocytic leukaemia protein content. Brain 2002; 125:1534–43
11. Hodges M, Tissot C, Howe K, Grimwade D, Freemont PS. Structure, organization, and dynamics of promyelocytic leukemia protein nuclear bodies. Am J Hum Genet 1998;63:297–304
12. Quignon F, De Bels F, Koken M, Feunteun J, Ameisen J-C, de Thé H. PML induces a novel caspase-independent death process. Nature Genet 1998;20:259–65
13. Wang Z-G, Ruggero D, Ronchetti S, et al. Pml is essential for multiple apoptotic pathways. Nature Genet 1998;20:266–72
14. Dyck JA, Maul GG, Miller WHJ, Chen JD, Kakizuka A, Evans RM. A novel macromolecular structure is a target of the promyelocyte-retinoic acid receptor oncoprotein. Cell 1994;76:333–43
15. Yasuda S, Inoue K, Hirabayashi M, et al. Triggering of neuronal cell death by accumulation of activated SEK1 on nuclear polyglutamine aggregations in PML bodies. Genes to Cells 1999;4:743–56
16. Yuen P, Baxter DW. The morphology of Marinesco bodies (paranucleolar colpuscles) in the melanin-pigmented nuclei of the brainstem. J Neurol Neurosurg Psychiatry 1963;26:178–83
17. Hirai S. Aging of the substantia nigra-histological and histochemical studies. Shinkei Shinpo (Advances in Neurology) 1965;12: 845–49
18. Shiraki H, Yamamoto T. Histochemical aspects of hepatocerebral diseases. Shinkei Shinpo (Advances in Neurology) 1960;5:73–101
19. Ono S, Inoue K, Mannen T, et al. Intracytoplasmic inclusion bodies of the thalamus and the substantia nigra, and Marinesco bodies in myotonic dystrophy: A quantitative morphological study. Acta Neuropathol 1989;77:350–56
20. Fujigasaki H, Uchihara T, Koyano S, et al. Ataxin-3 is translocated into the nucleus for the formation of intranuclear inclusions in normal and Machado-Joseph disease brains. Exp Neurol 2000;165: 248–56
21. Fujigasaki H, Uchihara T, Takahashi J, et al. Preferential recruitment of ataxin-3 independent of expanded polyglutamine: An immunohistochemical study on Marinesco bodies. J Neurol Neurosurg Psychiatry 2001;71:518–20
22. Uchihara T, Fujigasaki H, Koyano S, Nakamura A, Yagishita S, Iwabuchi K. Non-expanded polyglutamine proteins in intranuclear inclusions of hereditary ataxias—triple-labeling immunofluorescence study. Acta Neuropathol 2001;102:149–52
23. Moxley RT. Myotonic muscular dystrophy. In: Vinken PJ, Bruyn GW, Klawans HL, Rowland LP, DiMauro S, eds. Myopathies. Amsterdam: Elsevier, 1992: 209–59
24. Kiuchi A, Otsuka N, Namba Y, Nakano I, Tomonaga M. Presenile appearance of abundant Alzheimer's neurofibrillary tangles without senile plaques in the brain in myotonic dystrophy. Acta Neuropathol 1991;82:1–5
25. Abe K, Fujimura H, Toyooka K, et al. Involvement of the central nervous system in myotonic dystrophy. J Neurol Sci 1994;127: 179–85
26. Huber SJ, Kissel JT, Shuttleworth EC, Chakeres DW, Clapp LE, Brogan MA. Magnetic resonance imaging and clinical correlates of

intellectual impairment in myotonic dystrophy. Arch Neurol 1989; 46:536–40
27. Yoshida H, Kitamura K, Tanaka K, et al. Accelerated degradation of PML-retinoic acid receptor alpha (PML-RARA) oncoprotein by all-trans-retinoic acid in acute promyelocytic leukemia: Possible role of the proteasome pathway. Cancer Res 1996;56:2945–48
28. Frigo B, Scopsi L, Patriarca C, Rilke F. Silver enhancement of nickel-diaminobenzidine as applied to single and double immunoperoxidase staining. Biotech Histochem 1991;66:159–67
29. Bancher C, Lassman H, Budka H, et al. An antigenic profile of Lewy bodies: Immunocytochemical indication for protein phosphorylation and ubiquitination. J Neuropathol Exp Neurol 1989;48: 81–93
30. Rodrigues AA, Gregori L, Figueiredo-Pereira ME. Ubiquitin, cellular inclusions and their role in neurodegeneration. Trends Neurosci 1998;21:516–20
31. Perez MK, Paulson HL, Pendse SJ, Saionz SJ, Bonini NM, Pittman RN. Recruitment and the role of nuclear localization in polyglutamine-mediated aggregation. J Cell Biol 1998;143:1457–70
32. Anton LC, Schubert U, Bacik I, et al. Intracellular localization of proteasomal degradation of a viral antigen. J Cell Biol 1999;146: 113–24
33. Cummings CJ, Mancini MA, Antalffy B, DeFranco DB, Orr HT, Zoghbi HY. Chaperone suppression of aggregation and altered subcellular proteasome localization imply protein misfolding in SCA1. Nature Genet 1998;19:148–54

Received January 10, 2002
Revision received April 1, 2002
Accepted July 25, 2002

Experimental Neurology 178, 124–128 (2002)
doi:10.1006/exnr.2002.8028

Attenuated Nuclear Shrinkage in Neurons with Nuclear Aggregates—A Morphometric Study on Pontine Neurons of Machado–Joseph Disease Brains

Toshiki Uchihara,*[,1] Kiyoshi Iwabuchi,† Nobuaki Funata,‡ and Saburo Yagishita§

*Department of Neuropathology, Tokyo Metropolitan Institute for Neuroscience, Tokyo 183-8526, Japan; †Department of Neurology and Psychiatry and §Department of Pathology, Kanagawa Rehabilitation Center, Kanagawa, Japan; and ‡Department of Pathology, Tokyo Metropolitan Komagome Hospital, Tokyo, Japan

Received April 2, 2002; accepted July 31, 2002

Nuclear aggregates (NAs) and neurodegeneration in brains from patients with Machado–Joseph disease (MJD) are both triggered by pathological expansion of CAG/polyglutamine repeat in ataxin-3, but it remains to be clarified whether NA formation is associated with accelerated neurodegeneration. In an attempt to clarify a possible influence of NAs on neurons in human brains, we quantified the size and deformity of neuronal nuclei (those with or without NAs, separately) cross-sectioned on pontine preparations of autopsied brains from four patients with MJD and five controls. Nuclear shrinkage and deformity were more marked in MJD brains than in controls, and these changes were attenuated in neurons harboring NAs. NAs of MJD are presumably linked to a mechanism that attenuates rather than accelerates nuclear shrinkage and deformity. This finding leads us to consider that NAs are not necessarily toxic to neurons in diseased human brains. © 2002 Elsevier Science (USA)

Key Words: **intranuclear inclusions; neurodegeneration; ubiquitin; nuclear size; morphometry.**

INTRODUCTION

Because nuclear aggregates (NAs), found in brains with most CAG/polyglutamine expansion disorders, contain pathologically expanded polyglutamine and ubiquitin (23), it is now considered that these disorders share a mechanism underlying NA formation and neurodegeneration, both triggered by an expansion of CAG/polyglutamine. One of the pivotal questions, yet to be proved, is how NA formation is linked to neurodegeneration (17). If an expansion of CAG/polyglutamine leads to neurodegeneration and NA formation, morphological features of an individual neuron may be altered once it harbors NA. It is therefore essential to identify possible morphological changes in neurons and their relationship to NA in autopsied human brains. This is the first morphometric study on Machado–Joseph disease (MJD) which clarifies an influence of NA on nuclear size and deformity in the human brain.

MATERIALS AND METHODS

We examined autopsied brains from four unrelated Japanese cases of MJD and five controls without neurological disorders. As summarized previously (7), clinical and pathological features of these MJD cases were compatible with MJD, which was also confirmed by genetic analysis. Six-micrometer-thick formalin-fixed, paraffin-embedded sections were obtained from the mid-pons. Pontine nuclei were chosen because the size and appearance of the neurons are relatively homogeneous. This homogeneity made it easier to quantify and interpret their morphological changes. Moreover, the high frequency of NA in pontine neurons of MJD brains is another advantage in estimating its possible influence. Deparaffinized sections from the MJD cases were immunostained with an anti-ubiquitin antibody (rabbit polyclonal, 1:1000 Dako, Glostrup, Denmark) with diaminobenzidine as a chromogen and then stained lightly with hematoxylin. Ten rectangular microscopic fields (400×250 μm = 0.1 mm^2), chosen at random, were captured by a digital camera (D1, Nikon, Tokyo, Japan) connected to a microscope (BX-50, Olympus, Tokyo, Japan). Large cells harboring Nissl substances and a nucleus containing an identifiable nucleolus or ubiqutin-immunopositive NAs were identified as neurons. Although the correlation between nuclear size and cell size was apparent (6, 12) as shown in Fig. 1, we concentrated on nuclear morphology because changes in nuclear morphology (indentation or undulation of

[1] To whom correspondence should be addressed at Department of Neuropathology, Tokyo Metropolitan Institute for Neuroscience, 2-6 Musashi-dai, Fuchu, Tokyo 183-8526, Japan. Fax +81-42-321-8678. E-mail: uchihara@tmin.ac.jp.

0014-4886/02 $35.00

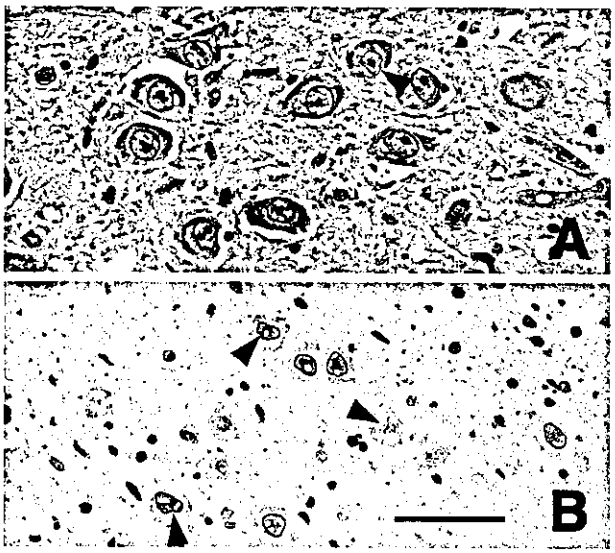

FIG. 1. Pontine neurons from a control case (A: hematoxlin–eosin stain) and an MJD case (B: ubiquitin immunostain counterstained with hematoxylin). The contour of the nucleus of each neuron is traced in black (in A and neurons with nuclear aggregates in B) or in white (neurons without nuclear aggregates in B). Undulations of the nuclear membrane were conspicuous (arrowheads in B) in MJD neurons with or without nuclear aggregates. Ubiquitin-immunopositive nuclear aggregates are indicated as white spots in B. (bar = 50 μm for A and B at the same magnification).

the nuclear membrane) have been reported to be characteristic of CAG repeat disorders (1, 18). The contour of the nuclear membrane and that of NAs, if present, of each neuron were traced on a digitizer coupled with a liquid crystal display (PL-400, Wacom, Saitama, Japan), as shown in Fig. 1. The "nuclear area" (cross-sectional area), "perimeter," "long axis," and "short axis" of the traced nuclear contours and "NA area" (cross-sectional area) of the traced NA contours were measured with NIH Image software (Version 1.62). Because an increase in nuclear size is partly attributable to the presence of NAs, the cross-sectional area of the nucleus not occupied by NA (nuclear area − NA area) was also calculated and analyzed. Nuclear deformity was assessed with long axis/short axis, the ratio of the two axes, and the "circularity index" (CI), defined by the ratio of two diameters, one of which was calculated from the perimeter (perimeter/2π) and the other from the area (the square root of (area/π)). CI is equal to 1 if the traced nuclear contour is a perfect circle. Both ratio and CI are expected to be increased with increasing severity of nuclear deformities, such as elongation, distortion, or undulations of the nuclear membrane. Differences in these parameters between the groups; nuclei with NA (NA+ group), those without NA (NA− group), both from MJD cases (MJD total group, including both NA+ and NA− groups) and controls, were estimated with ANOVA or Student's t test.

RESULTS

Table 1 shows the demographic data for the patients and the neuronal count for each case. Although the mean of the neuronal counts (representing the mean of "packing density") of the MJD group (135.5/mm^2) was smaller than that of the controls (160.2/mm^2), this difference did not reach statistical significance ($P > 0.1$ after the Mann–Whitney U test). Morphological data assembled from each group are shown in Table 2. The nuclear area, perimeter, long axis, and short axis were significantly smaller in the MJD total group (e.g., the mean of the nuclear area, 60.9 μm^2) than in the controls (e.g., the mean nuclear area, :90.5 μm^2, $P < 0.0001$ by Student's t test). Inverted histograms in Fig. 2 show that the size distribution of the cross-sectional area of the nucleus (nuclear area) of the MJD total group (filled bars) is smaller than that of the controls

TABLE 1

Neuronal Counts (/mm^2) with or without Nuclear Aggregates

Case	Age at onset/ death (years)	Sex	+	−	Total
MJD case 1	25/42	F	41	76	117
MJD case 2	27/40	F	43	87	130
MJD case 3	37/51	F	83	108	191
MJD case 4	42/64	F	55	49	104
				Mean (MJD) 135.5*	
Control	/25	M	0	140	140
Control	/25	F	0	174	174
Control	/40	F	0	154	154
Control	/44	M	0	157	157
Control	/45	F	0	176	176
				Mean (normal) 160.2	

Note. +, Number of neurons with nuclear aggregates (NAs); −, number of neurons without NAs; total, sum of − and +; MJD, Machado–Joseph disease; F, female; M, male.

* Not significantly smaller than the control group ($P > 0.1$, after Mann–Whitney U test).

TABLE 2

Morphometric Parameters of Pontine Neurons of Controls and Machado–Joseph Disease Cases

Group (n)	Controls (5)	Total(MJD)	MJD (4) NA (+)	NA (−)
Number of neurons	801	543	222	321
Nuclear area (μm^2)	90.5 ± 0.7	60.9 ± 0.8*	71.3 ± 1.1**	53.8 ± 0.9***
(Nuclear area - NA area (μm^2))		(59.1 ± 0.7*	66.7 ± 1.1**)	
Perimeter (μm)	36.3 ± 0.1	30.2 ± 0.2*	32.4 ± 0.2**	28.7 ± 0.2***
Long axis (μm)	12.00 ± 0.05	10.23 ± 0.07*	10.86 ± 0.08**	9.80 ± 0.09***
Short axis (μm)	9.54 ± 0.04	7.47 ± 0.07*	8.30 ± 0.09**	6.89 ± 0.08***
Long axis/short axis	1.27 ± 0.01	1.41 ± 0.01*	1.34 ± 0.02**	1.46 ± 0.02***
Circularity index	1.085 ± 0.001	1.110 ± 0.002*	1.093 ± 0.003**	1.119 ± 0.003***

Note. Expressed as the mean ± SE; MJD; Machado–Joseph disease; n, number of cases; total, all neurons from MJD cases; NA(+), neurons with nuclear aggregates (NA) from MJD cases; NA(−), neurons without nuclear aggregates from MJD cases; * $P < 0.0001$ compared with normal group (Student's t test); ** $P < 0.001$ when compared with normal; *** $P < 0.0001$ when compared with inclusion(+) (by ANOVA, Fisher's PLSD at 1% probability).

(unfilled bars). Nuclear size (estimated with nuclear area, perimeter, long axis, and short axis) was smaller in the NA− group than in the NA+ group. In other words, neuronal nuclei of the NA+ group were less atrophic than those of the NA− group ($P < 0.0001$ by ANOVA, Fisher's at 1% probability). The upper histograms in Fig. 2 demonstrate this difference between the NA+ group (unfilled bars) and the NA− group (filled bars) in nuclear area. The difference between NA+ (mean = 71.3 μm^2) and NA− (mean = 53.8 μm^2) groups in the cross-sectional area of the nucleus remained significant even when the NA area was subtracted from the nuclear area to yield by calculation the nuclear area − NA area (mean = 66.7 μm^2, NA+ group), which represented the cross-sectional area of the nucleus not occupied by NA. Although both parameters for nuclear deformity (ratio and CI) were increased in the MJD group, nuclear deformity was more marked in the NA− group (Table 2 Fig. 3).

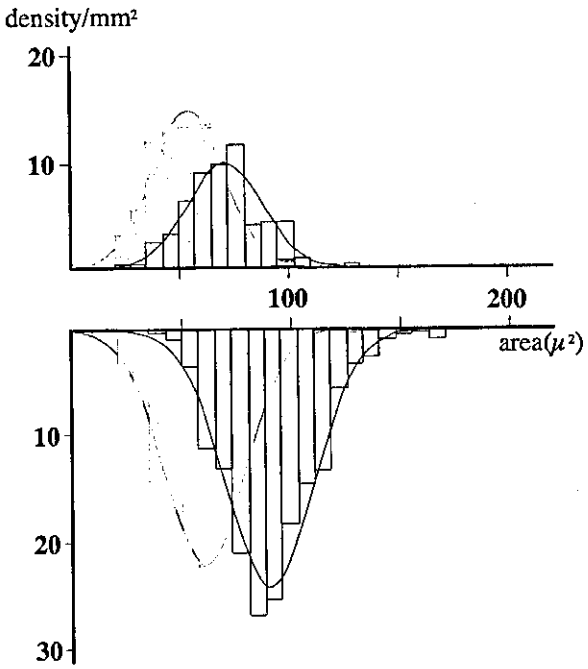

FIG. 2. Size distribution of the nucleus of the pontine neurons of MJD and normal control cases. Cross-sectional area of each nucleus estimated as the "nuclear area" in square micrometers is expressed on the abscissa. The ordinate represents the relative frequency of each size expressed as density per square millimeter. The lower inverted histograms represent controls (unfilled bars with a black line) and the MJD group as a whole (MJD total group, bars filled with gray). The upper histograms indicate the MJD group with nuclear aggregates (NA+ group, unfilled bars with a black line) or without nuclear aggregates (NA− group, bars filled with gray).

DISCUSSION

After identification of the pathological expansion of CAG/polyglutamine tracts linked to several forms of hereditary ataxias including MJD, these genetic abnormalities have been considered responsible for both neurodegeneration and NA formation, one of the pathological hallmarks for most of these CAG/polyglutamine repeat disorders. It is, however, still a matter of considerable debate how NA is related to neurodegeneration. Because degenerative processes evolve slowly and usually take several years or even decades, progressive decrease in cell size (cellular atrophy), considered to represent a stage preceding cell death, is a principal feature of neurodegeneration regardless of etiology. In the present study we confirmed that this atrophic feature is also shared with pontine neurons in MJD cases. Sorting the neurons into two groups, those with (NA+ group) or without (NA− group) NA, however, unexpectedly clarified that neurons harboring NA exhibited less shrinkage than those not harboring NA.

In vitro, as well as *in vivo,* studies have provided conflicting evidence regarding possible roles of NA formation and its relationship to neurodegeneration. Al-

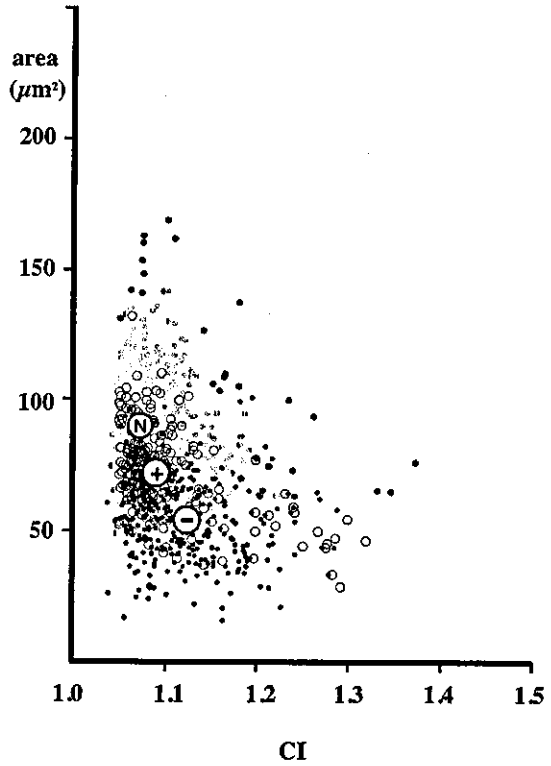

Fig. 3. Relationship between nuclear size (nuclear area on the ordinate in square micrometers) and the deformity of the each nucleus (circularity index (CI) on the abscissa). CI is equal to 1 if the nucleus is a perfect circle and increases if the nucleus is deformed by elongation or undulation. Gray dots, normal group; black dots, NA- group; open circles, NA+ group. Mean values for each group are plotted as N, normal group; −, NA− group; and +, NA+ group in the scattergram.

though both neurodegeneration and NA formation in transgenic models for Huntington's disease (HD) are inducible by sustained expression of the huntingtin fragment carrying expanded polyglutamine (22), or possibly suppressed by inhibition of caspase-1 (13), these two features could be discrepant (8, 9, 14, 21) or even inversely related in cultured cells transfected with the huntingtin gene carrying an expanded CAG repeat (16). Postmortem observation of human brains with HD (11) or neuronal intranuclear hyaline inclusion disease (NIHID) (20) demonstrated a similar discrepancy between neuronal depletion and NA formation. Moreover, we recently confirmed the absence of NAs in cerebellar Purkinje cells in an autopsy series of hereditary ataxias (spinocerebellar ataxia type-1, -2, and -3 and dentatorubral pallidoluysian atrophy (DRPLA)) (10). At least two interpretations, absolutely conflicting with each other, have been proposed to explain these data. Neurons harboring NAs may be more susceptible to the atrophic process, preferentially leaving those not containing NAs relatively unaffected. One may, then, expect that neurons with NAs, preferentially involved in neurodegeneration, are more atrophic. The other possibility is that neurons containing NAs may be relatively more resistant (14). If this is the case, it should be neurons not harboring NAs that are more susceptible and their atrophic process is expected to be more exaggerated. The latter possibility is now shown to be more plausible in pontine neurons of MJD brains because the present study demonstrated that neuronal nuclei harboring NA were larger than those not harboring NA, whereas pontine neurons of MJD brains, regardless of the presence of NAs, are more atrophic than those of controls. This larger size of neuronal nuclei in the NA+ group relative to the NA− group remained significant even when the NA area was subtracted from the nuclear area. This means that an insertion of NA is not enough to wholly explain this difference, and other mechanisms linked to NAs may underlie this relative increase in nuclear size, linked to NAs.

Nuclear deformity of pontine neurons in MJD brains, quantified as an increase in ratio and CI, is potentially linked to its shrinkage. The present study demonstrated that the severity of nuclear deformity was more apparent in the NA− group, whereas nuclear deformity seen in the NA+ group was as attenuated as its nuclear shrinkage was. Apparent indentation of the nuclear membrane has been observed even in normal neurons (15) and its pathological increase has been described in human brains with DRPLA (18), HD (1), and its animal model (4). Although our observation based on light microscopy failed to identify deep indentations in the nuclear membrane, an increase in ratio and CI observed in MJD neurons may represent similar pathological processes, which are shared with these neurological disorders linked to pathological expansion of CAG/polyglutamine repeat disorders.

Although the cellular mechanism, which may link NA formation and neurodegeneration, remains to be clarified, downregulation of the ubiquitin–proteasome pathway has been found to suppress NA formation and accelerate cell death *in vitro* in parallel (3). This inverse relationship between cell death and NA formation through the ubiquitin–proteasome pathway suggests that NA formation is linked to a possible intrinsic neuroprotective mechanism mediated by ubiquitin. Our previous studies demonstrated that ubiquitin was localized to the periphery of each NA in MJD (5) and in NIHID (19) brains. These findings are explained if NA formation, mediated by ubiquitin, is associated with a mechanism counteracting neuronal shrinkage in MJD, as was reported in SCA1 transgenic mice (3). A recent morphometric study on DRPLA brains demonstrated that cerebellar granule cells containing NAs were larger than those not containing NAs (18). It is probable that this anti-atrophic influence of NA is common to MJD and DRPLA brains. This implies that neurons are inherently equipped with machinery that counteracts shrinkage, triggered simultaneously during NA forma-

tion. It is essential to clarify whether this anti-atrophic influence of NA is to be extrapolated to other disorders with ubiquitin-immunopositive NAs in human brains. It is more important to clarify the molecular mechanism that governs NA formation or neuronal atrophy together or separately. This will give a rational basis for treatment that may retard or even reverse neurodegeneration by activating or modulating this machinery.

ACKNOWLEDGMENTS

This work was supported partly by grants from the Ministry of Health and Welfare (KI) and from the Japan Society for the Promotion of Science/INSERM (TU). The authors are grateful to Mr. Ray Cowan for reading the manuscript.

REFERENCES

1. Bots, G. T. A. M., and G. W. Bruyn. 1981. Neuropathological changes of the nucleus accumbens in Huntington's chorea. *Acta Neuropathol.* **55:** 21–22.
2. Cummings, C. J., M. A. Mancini, B. Antalffy, D. B. DeFranco, H. T. Orr, and H. Y. Zoghbi. 1998. Chaperone suppression of aggregation and altered subcellular proteasome localization imply protein misfolding in SCA1. *Nat. Genet.* **19:** 148–154.
3. Cummings, C. J., E. Reinstein, Y. Sun, B. Antalffy, Y.-H. Jiang, A. Ciechanover, H. T. Orr, A. L. Beaudet, and H. Y. Zoghbi. 1999. Mutation of the E6-AP ubiquitin ligase reduces nuclear inclusion frequency while accelerating polyglutamine-induced pathology in SCA1 mice. *Neuron* **24:** 879–892.
4. Davies, S. W., M. Turmaine, B. A. Cozens, M. DiFiglia, A. H. Sharp, C. A. Ross, E. Scherzinger, E. E. Wanker, L. Mangiarini, and G. P. Bates. 1997. Formation of neuronal intranuclear inclusions underlies the neurological dysfunction in mice transgenic for the HD mutation. *Cell* **90:** 537–548.
5. Fujigasaki, H., T. Uchihara, S. Koyano, K. Iwabuchi, S. Yagishita, T. Makifuchi, A. Nakamura, K. Ishida, S. Toru, S. Hirai, K. Ishikawa, T. Tanabe, and H. Mizusawa. 2000. Ataxin-3 is translocated into the nucleus for the formation of intranuclear inclusions in normal and Machado–Joseph disease brains. *Exp. Neurol.* **165:** 248–256.
6. Hertwig, R. 1903. Ueber Korrelation von Zell- und Kerngrösse und ihre Bedeutung für die deschlechtliche Differenzierung und die Teilung der Zelle. *Biol. Zbl.* **23:** 49–119.
7. Iwabuchi, K., K. Tsuchiya, T. Uchihara, and S. Yagishita. 1999. Autosomal dominant spinocerebellar degenerations. Clinical, pathological and genetic correlations. *Rev. Neurol. (Paris)* **155:** 255–270.
8. Kim, M., H. S. Lee, G. LaForet, C. McIntyre, E. J. Matin, P. Chang, T. W. Kim, M. Williams, P. H. Reddy, D. Tagle, F. M. Boyce, L. Won, A. Heller, N. Aronin, and M. DiFiglia. 1999. Mutant huntingtin expression in clonal striatal cells: Dissociation of inclusion formation and neuronal survival by caspase inhibition. *J. Neurochem.* **19:** 964–973.
9. Klement, I. A., P. J. Skinner, M. D. Kaytor, H. Yi, S. M. Hersch, H. B. Clark, H. Y. Zoghbi, and H. T. Orr. 1998. Ataxin-1 nuclear localization and aggregation: role in polyglutamine-induced disease in SCA1 transgenic mice. *Cell* **95:** 41–53.
10. Koyano, S., K. Iwabuchi, S. Yagishita, Y. Kuroiwa, and T. Uchihara. 2002. Paradoxical absence of nuclear inclusion in cerebellar Purkinje cells of hereditary ataxias linked to CAG expansion. *J. Neurol. Neurosurg. Psychiatry* **73:** 453–455.
11. Kuemmerle, S., C.-A. Gutekunst, A. M. Klein, X.-J. Li, S.-H. Li, M. F. Beal, S. M. Hersche, and R. J. Ferrante. 1999. Huntingtin aggregates may not predict neuronal death in Huntington's disease. *Ann. Neurol.* **46:** 842–849.
12. Montagne, J. 2000. Genetic and molecular mechanisms of cell size control. *Mol. Cell. Biol. Res. Commun.* **4:** 195–202.
13. Ona, V. O., M. Li, J. P. Vonsattel, L. J. Andrews, S. Q. Khan, W. M. Chung, A. S. Frey, A. S. Menon, X.-J. Li, P. E. Stieg, J. Yuan, J. B. Penney, A. B. Young, J.-H. J.Cha, and R. M. Friedlander. 1999. Inhibition of caspase-1 slows disease progression in a mouse model of Huntington's disease. *Nature* **399:** 263–267.
14. Ordway, J. M., S. Tallaksen-Greene, C.-A. Gutekunst, E. M. Bernstein, J. A. Cearley, H. W. Wiener, L. S. Dure IV, R. Lindsey, S. M. Hersch, R. S. Jope, R. L. Albin, and P. J. Detloff. 1997. Ectopically expressed CAG repeats cause intranuclear inclusions and a progressive late onset neurological phenotype in the mouse. *Cell* **91:** 753–763.
15. Roos, R. A. C., and G. T. A. M. Bots. 1983. Nuclear membrane indentations in Huntington's chorea. *J. Neurol. Sci.* **61:** 37–47.
16. Saudou, F., S. Finkbeiner, D. Devys, and M. E. Greenberg. 1998. Huntingtin acts in the nucleus to induce apoptosis but death does not correlate with the formation of intranuclear inclusions. *Cell* **95:** 55–66.
17. Sisodia, S. S. 1998. Nuclear inclusions in glutamine repeat disorders: Are they pernicious, coincidental, or beneficial? *Cell* **95:** 1–4.
18. Takahashi, H., S. Egawa, Y.-S. Piao, S. Hayashi, M. Yamada, K. Oyanagi, and S. Tsuji. 2001. Neuronal nuclear alterations in dentatorubral-pallidoluysian atrophy: Ultrastructural and morphometric studies of cerebellar granule cells. *Brain Res.* **919:** 12–19.
19. Takahashi, J., T, Fukuda, J. Tanaka, H. Fujigasaki, M. Minamitani, and T. Uchihara. 2000. Neuronal intranuclear hyaline inclusion disease with polyglutamine immunoreactive inclusions. *Acta Neuropathol.* **99:** 589–594.
20. Takahashi, J., J. Tanaka, K. Arai, N. Funata, T. Hattori, T. Fukuda, H. Fujigasaki, and T. Uchihara. 2001. Recruitment of non-expanded polyglutamine proteins in intranuclear aggreages of neuronal intranuclear hyaline inclusion disease. *J. Neuropathol. Exp. Neurol.* **60:** 369–376.
21. Watase, K., E. J. Weeber, B. Xu, B. Antalffy, L. Yuva-Paylor, K. Hashimoto, M. Kano, R. Atkinson, Y. Sun, D. L. Armstrong, J. D. Sweatt, H. T. Orr, R. Paylor, and H. Y. Zoghbi. 2002. A long CAG repeat in the mouse sca1 locus replicates SCA1 features and reveals the impact of protein solubility on selective neurodegeneration. *Neuron* **34:** 905–919.
22. Yamamoto, A., J. J. Lucas, R. and Hen. 2000. Reversal of neuropathology and motor dysfunction in a conditional model of Huntington's disease. *Cell* **101:** 57–66.
23. Zoghbi, H. Y., and H. T. Orr. 2000. Glutamine repeats and neurodegeneration. *Annu. Rev. Neurosci.* **2000:** 217–47.

Acta Neuropathol (2003) 105:103–108
DOI 10.1007/s00401-002-0614-9

REGULAR PAPER

Toshiki Uchihara · Junichi Tanaka · Nobuaki Funata
Kimihito Arai · Takamichi Hattori

Influences of intranuclear inclusion on nuclear size – morphometric study on pontine neurons of neuronal intranuclear inclusion disease cases

Received: 29 April 2002 / Revised: 8 August 2002 / Accepted: 8 August 2002 / Published online: 13 September 2002

Abstract In looking for a possible influence of nuclear inclusions (NIs) on neurodegeneration in human brains, we quantified morphological features of pontine neurons of three unrelated cases of neuronal intranuclear inclusion disease (NIID) and five control cases. Cross-sectional area of each neuronal nucleus and the indices for its deformity (long axis/short axis and circularity index defined as deviation from the perfect circle) were measured on pontine sections and their relation to NIs was statistically analyzed. Cross-sectional area of neuronal nuclei harboring ubiquitin-immunopositive NIs was significantly larger (110.6±1.6 μm^2, mean ± SE), while that of nuclei not harboring NIs was smaller (77.8±1.5 μm^2) than that in controls (90.5±0.7 μm^2). This difference remained significant even when the cross-sectional area occupied by NIs was subtracted from that of the nucleus harboring the NI (97.4±1.5 μm^2). This could hardly be explained if nuclear shrinkage is accelerated in the presence of NI. On the contrary, NI formation in pontine neurons of NIID might be linked, either directly or indirectly, to a mechanism, which counteracts rather than accelerates nuclear shrinkage. Because nuclear deformity was apparent even in neurons with NIs, whose nuclei were significantly larger than controls, the nuclear deformity is not secondary to its shrinkage and represents another aspect of neurodegeneration independent of nuclear shrinkage. Association of NIs to neurons of larger nuclear size in NIID brain indicates that NIs are not necessarily toxic to neurons.

Keywords Neuronal intranuclear inclusion disease · Intranuclear inclusions · Ubiquitin · Morphometry · Neurodegeneration

T. Uchihara (✉)
Department of Neuropathology,
Tokyo Metropolitan Institute for Neuroscience,
2-6 Musashi-dai, Fuchu, Tokyo, 183-8526 Japan
e-mail: uchihara@tmin.ac.jp,
Tel.: +81-42-3253881/4712, Fax: +81-42-3218678

J. Tanaka
Division of Neuropathology,
Jikei University School of Medicine,
3-25-8 Nishishimbashi, Minato-ku, Tokyo, 105-8461 Japan

N. Funata
Department of Pathology,
Tokyo Metropolitan Komagome Hospital,
3-18-22 Hon-komagome, Bunkyo-ku, Tokyo, 113–8677 Japan

K. Arai · T. Hattori
Department of Neurology, Chiba University,
1-8-1 Inohana, Chuo-ku, Chiba, 260–8670 Japan

Introduction

Neuronal intranuclear inclusion disease (NIID) represents a group of neurodegenerative disorders characterized by the presence of ubiquitin-immunopositive nuclear inclusions (NIs) possibly related to neurodegeneration. Because ubiquitin-immunopositive NIs are also found in brains from patients with most of CAG/polyglutamine expansion disorders [36], it is likely that these disorders share, at least partly, a mechanism of neurodegeneration linked to NI formation [5]. One of the principal questions, yet to be addressed, is whether the presence of NI is linked to accelerated neurodegeneration or not [24]. We previously examined brains obtained at autopsy from three unrelated Japanese patients with NIID and found that a high frequency of NIs was inversely correlated with the severity of tissue damage [28, 29]. This inverse correlation is hardly explained if the presence of NI is directly linked to accelerated neurodegeneration [28]. Because conventional interpretation of histological sections deals with accumulated sequel after a long period of degeneration, it is difficult to specify how a particular NI exerts its influence on the neuron actually harboring the NI at a given time, for example, at autopsy. The present study is an extension of the previous one [29] and focuses on morphological changes of each neuron. Given that a cellular mechanism leading to neuronal death is influenced by NI formation, one may expect that morphological aspects during this degenerative process (usually atrophy) of an individual neuron may be altered once it harbors NIs. To

Table 1 Density (n/mm^2) of neurons with or without NIs (*FH* family history, *N* negative, *P* positive, *NI* intranuclear inclusion, + number of neurons with NIs, – number of neurons without NIs, *total*: sum of – and +, *NIID* neuronal intranuclear inclusion disease)

	Age at onset/ death (years)	FH	Sex	+	–	Total
NIID cases						
1 [28]	12/25	N	F	138	65	203
2 [16]	11/26	N	M	126	65	191
3 [29]	25/41	P	M	73	85	158
				Mean (NIID) 184.0^{NS}		
Diagnosis of the control cases						
AIDS	/25		M	0	140	140
Myelodysplastic syndrome	/25		F	0	174	174
Cervical carcinoma	/40		F	0	154	154
Phyllodes tumor	/44		M	0	157	157
Myeloma	/45		F	0	176	176
				Mean (control) 160.2^{NS}		

^{NS}No significant difference in total number of neurons between NIID and normal groups (P>0.1, Mann-Whitney U test)

address this question, we quantified morphological aspects (the nuclear size and deformity) of each pontine neuron in the three autopsy cases of NIID and of five control cases. Possible influences of NIs on these morphological parameters provided an insight into this degenerative process characterized by NIs. This is the first morphometric study based on human brains with NIID, and has provided cellular evidence that NI formation is linked to an increase in nuclear size rather than shrinkage.

Materials and methods

Patients and controls

Three unrelated Japanese cases of NIID [8, 28, 29] were enrolled in this study. Clinical pictures of these cases were summarized previously [29]. Although NIs of these three cases were immunopositive for ataxin-2, ataxin-3 and TATA box-binding protein as reported [15, 29, 31], they were not associated with pathological expansion of CAG repeat in any of these or other known genes linked to hereditary ataxias, as we confirmed previously [29]. The ultrastructure of NIs of these cases was described previously and was indistinguishable from those described in the literature [29]. Although their clinical features were variable, regional distribution and prevalence of NIs were found to be inversely correlated with the severity of tissue damage as estimated semiquantitatively [29]. Some of the glial cells also contained aggregates in their nuclei [29]. Five normal control cases of the same age range (age at death 25–45 years) without neurological disorders were examined for comparison (Table 1).

Histological sections, staining, data acquisition and analysis

Paraffin-embedded formalin-fixed sections, 6 μm thick, were obtained from the mid-pons. Pontine nuclei were chosen because the size and appearance of the neurons are relatively homogeneous. This homogeneity made it easier to quantify and interpret their morphological changes. Moreover, the high frequency of NIs in pontine neurons of NIID brains is another advantage in estimating its possible influence. Deparaffinized sections from the NIID cases were immunostained with an anti-ubiquitin antibody (rabbit polyclonal, 1:1,000 DAKO, Glostrup, Denmark) with diaminobenzidine as a chromogen and were then stained lightly with hematoxylin. Ten rectangle microscopic fields (400×250 μm=0.1 mm^2), chosen at random, were captured by a digital camera (D1, Nikon, Tokyo, Japan) connected to a microscope (BX-50, Olympus, Tokyo, Japan). Large cells harboring Nissl substances and a nucleus harboring an identifiable nucleolus were identified as neurons. Although the correlation between nuclear size and cell size was apparent [9, 17] as shown in Fig. 1, we concentrated on the nucleus of neurons because changes in its morphology (indentation or undulation of the nuclear membrane) have been reported to be characteristic of CAG repeat disorders [1, 27] with NIs. The contour of the nuclear membrane and that of NIs, if present, of each neuron were traced on a digitizer coupled with a liquid crystal display (PL-400, Wacom, Saitama, Japan), as shown in Fig. 1. The nuclear area (cross-sectional area), perimeter, long axis and short axis of each traced nuclear contour and NI area (cross-sectional area) of each traced NI contour were measured with the software, NIH-Image (Version 1.62). Because an increase in nuclear size is

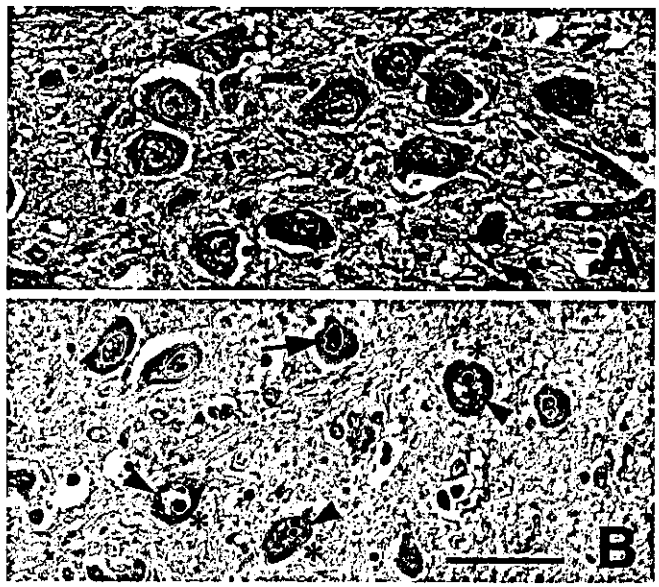

Fig. 1 Pontine neurons from a normal control case (**A** hematoxylin-eosin staining) and a NIID case (**B** ubiquitin immunostaining counterstained with hematoxylin). The contour of the nucleus of each neuron is traced in *black* (in **A** and neurons with NIs, as indicated by asterisks in **B**) or in *white* (neurons without NIs in **B**). The contours of NIs are traced in *white* (neurons indicated by *asterisks* in **B**). Undulations of the nuclear membrane are most conspicuous (*arrow* in **B**) in NIID neurons without NIs. Although some of the neurons of the normal control cases exhibited a similar but slighter deformity (*small arrowhead* in **A**), these changes were readily detectable even in neurons harboring NIs without atrophy (*arrowheads* in **B**) (*NIID* neuronal intranuclear inclusion disease, *NI* nuclear inclusion). *Bar* 50 μm

Table 2 Morphometric parameters of pontine neurons of the normal and NIID cases. Expressed as mean ± SE (*n* number of cases, *total* all neurons from NIID cases, *inclusion+* neurons with NI from NIID cases, *inclusion–* neurons without NI from NIID cases, *Nuclear area–NI area* nuclear area not occupied by NI, *CI* circularity index)

	Normal (n=5)	NIID (n=3)		
		Total	Inclusion+	Inclusion–
No. of neurons	801	513	298	215
Nuclear area (μm²)	90.5±0.7	96.8±1.3*	110.6±1.6**	77.8±1.5**
Nuclear area–NI area (μm²)		89.2±1.2^{NS}	97.4±1.5**	77.8±1.5**
Perimeter (μm)	36.3±0.1	38.2±0.3*	40.5±0.3**	35.0±0.3**
Long axis (μm)	12.00±0.05	12.85±0.08*	13.55±0.10**	11.87±0.11(*)
Short axis (μm)	9.54±0.04	9.44±0.09^{NS}	10.30±0.10**	8.26±0.11**
Long axis/short axis	1.27±0.01	1.40±0.01*	1.35±0.01**	1.49±0.02**
CI	1.085±0.001	1.111±0.003*	1.095±0.002#	1.132±0.005**

*P<0.0001 compared with the normal group (Student's t-test), **P<0.0001 when compared with the normal group, (*)P<0.0001 compared with inclusion+ group, but not significantly different from the normal group, ^{NS}: not significant when compared with the normal group, #P=0.0008 when compared with the normal group (by ANOVA, PLSD of Fisher at 1% probability)

partly attributable to the presence of NIs, the cross-sectional area of the nucleus not occupied by NI (nuclear area–NI area) was also calculated and analyzed. Nuclear deformity was assessed with long axis/short axis, the ratio of the two axes, and the circularity index (CI) defined by the ratio of two diameters, one of which was calculated from the perimeter (perimeter/2π) and the other from the area [the square root of (area/π)]. CI is equal to 1 if the traced nuclear contour is a perfect circle. Both ratio and CI are expected to increase with increasing severity of nuclear deformity, such as elongation, distortion or undulations of the nuclear membrane. Differences in these parameters between the groups, i.e., nuclei harboring NIs (Inclusion+ group), those not harboring NI (Inclusion– group), both from NIID cases (NIID total group, which includes both Inclusion+ and Inclusion- groups) and controls, were estimated with ANOVA or Student's t-test.

Results

Packing density of pontine neurons

Table 1 shows the demographic data of the patients and neuronal counts of each case. Although the mean of neuronal counts (representing the mean of "packing density") of NIID group (184.0/mm²) was greater than that of normal group (160.2/mm²), non-parametric comparison of neuronal counts between NIID and normal groups failed to reveal significant difference between the groups (P>0.1 after Mann-Whitney U test).

Nuclear size of pontine neurons

Morphological data assembled from each group are shown in Table 2. Nuclear area, perimeter and long axis were significantly larger in NIID as a whole (mean of nuclear area 96.8 μm², NIID total group in Table 2) than in normal group (mean of nuclear area 90.5 μm², P<0.0001 by Student's-t test). This difference was due to larger cross-sectional area of nucleus of Inclusion+ group (mean of nuclear area 110.6 μm²), whereas that of Inclusion– group was significantly smaller (mean of nuclear area 77.8 μm²) than that of normal group. This increase in nuclear cross-sectional area of Inclusion+ group relative to normal group remained significant even when nuclear area

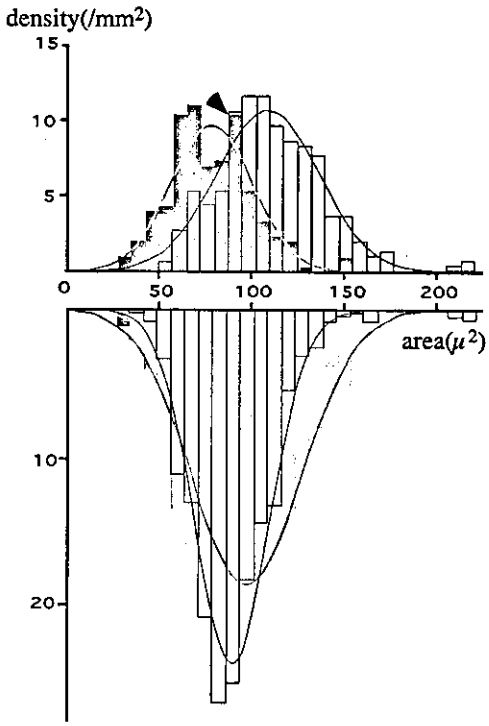

Fig. 2 Distribution of the nuclear cross-sectional area of the pontine neurons of NIID and normal control cases. Nuclear size estimated as nuclear area in μm² is expressed along the *abscissa*. The relative frequency of each size range is expressed along the *ordinate* as density/mm². The *lower inverted histograms* represent the normal control group (*unfilled bars* with *black lines*) and NIID group as a whole (NIID total group, *filled bars* with *gray columns*), which exhibits bimodal peaks. The *upper histograms* represent NIID group with NIs (Inclusion+ group, *unfilled bars* with *black lines*), and without NIs (Inclusion– group, *filled bars* with *gray columns*). Note the *upper peak* in the Inclusion– group (*arrowhead*), which may represent some of the neurons harboring NIs not included in the sectioned plane

was replaced by nuclear area–NI area (mean 97.4 μm²), representing nuclear cross-sectional area not occupied by NIs. The size distribution of nuclear area is shown in Fig. 2. Although the normal group (Figs. 1A, 2) exhibited a normal distribution with a single peak, the distribution of NIID total group was bimodal. Its upper peak corresponded to Inclusion+ group (Fig. 1B) and its lower peak corresponded to Inclusion– group, which exhibited bimodal distribution with two lower peaks around 70 and 90 μm² (mean 77.8 μm²). There was no correlation between nuclear area and NI area (R^2=0.159).

Nuclear deformity and its relation to nuclear size

Although the long axis of Inclusion– group was not statistically different from that of the normal group, the short axis was significantly smaller in Inclusion– group. This accounts for a significant increase in the ratio (long axis/short axis, Table 2) in Inclusion– group (Fig. 1B), also seen in Inclusion+ group (Fig. 1B), indicating that the shape of neuronal nuclei of NIID is more or less elongated or distorted (Fig. 1B) irrespective of the presence of NIs or nuclear size. Although undulations of the nuclear membrane were most conspicuous in Inclusion– group (Fig. 1B), similar nuclear deformity was detectable even in normal group (Fig. 1A). Nuclear deformity was also evaluated as an increase in CI and its relation to nuclear area is shown as a scattergram (Fig. 3). Because a significant fraction of neurons of Inclusion+ group exhibited these deformities (Figs. 1B, 3), even the Inclusion+ group was associated with a significant increase in CI, and ratio (long axis/short axis) compared with the normal group (Table 2). This nuclear deformity was, however, more marked in Inclusion– group. Compared with the normal group, neurons in the Inclusion+ group clustered in the upper zone (larger nuclear area), while those of Inclusion– group clustered in the lower zone (smaller nuclear area) (Fig. 3). Both Inclusion+ and Inclusion– groups, however, clustered in the area with increased CI (right side) compared with the normal group.

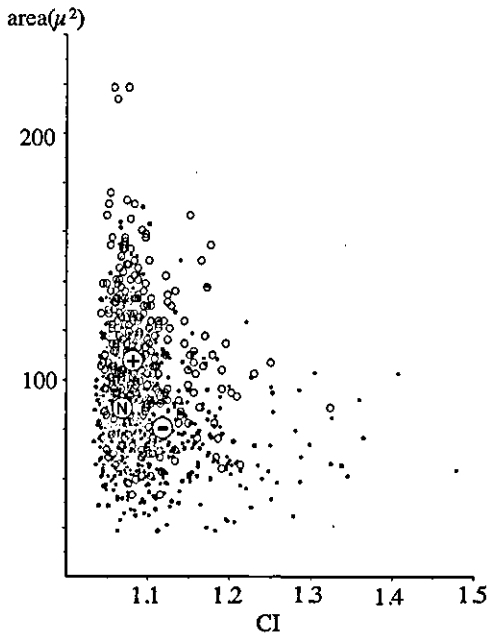

Fig. 3 Relation between nuclear size (nuclear area along the *ordinate* in μm²) and deformity of the nucleus (CI along the *abscissa*). CI is equal to 1 if the contour of a nucleus is a perfect circle and is expected to be increased if the nucleus is deformed. *Gray dots*: Normal group, *black dots*: Inclusion– group, *open circles*: Inclusion+ group. Mean values of each group are indicated as *N*, – and + in the scattergram, respectively (*CI* circularity index)

Discussion

Previous reports on NIID suggested that the presence of NIs was not necessarily linked to neuronal loss, because numerous NIs were found even in areas without discernible neurodegeneration [8, 16, 18, 23, 25, 26, 30, 34]. The lack of a significant decrease in the packing density of pontine neurons of NIID, which we demonstrated in the present study, confirmed these observations. In our previous report on the same three Japanese cases of NIID, we semiquantitatively evaluated the severity of tissue damage, which was found inversely correlated with the frequency of NIs. At least two interpretations, absolutely conflicting with each other, are possible to explain this inverse relationship. Neurons harboring NIs may be more susceptible to degeneration by way of atrophy, leaving after some period those not harboring NIs. One may, then, expect that the nuclear size of neurons harboring NIs, if preferentially involved in this process, would be smaller. However, this is contrary to the findings of the present study. The opposite interpretation is that neurons harboring NIs may be relatively more resistant. Neurons not harboring NIs, therefore, are more susceptible and more severely involved in the atrophic process. Our previous study [29], which estimated the severity of tissue damage by a conventional method, however, was not sufficient to settle this argument between these opposing interpretations. The more precise and sophisticated morphometric approach used in the present study showed that the latter possibility is more plausible since the cross-sectional area of neurons harboring NIs was found to be larger than that of neurons not harboring NIs. Because this difference remained significant even when NI area was subtracted from nuclear area, as the inserted NI could only account for part of this increase. This means that mechanisms other than simple insertion of NI may underlie the increase in nuclear size, which is also linked to the presence of NI.

Observation on a single histological plane, however, does not assure the absence of NIs in the neuron under examination, because neurons classified into Inclusion– group might contain NIs elsewhere not included in the section. If neuronal nuclei harboring NIs were smaller than those not harboring NIs, this possible failure to identify NIs not included in the two-dimensional plane might

have led to an underestimation of the nuclear size of neurons in Inclusion– group, which might have obscured the interpretation. However, since the present study indicated the opposite direction, by showing that neuronal nuclei of Inclusion+ group were larger than those of Inclusion– group, it is justified to conclude from this two-dimensional study that nuclear size of neurons harboring NIs is larger than that of neurons not harboring NIs. It is, therefore, reasonable to assume that the upper peak (Fig. 2) of the histogram for Inclusion– group represents a group of neurons which harbor NIs in reality but was classified as Inclusion– group, because the NIs were not included in the section. If NI formation is accompanied by a gradual increase in nuclear size, or disappearance of NI is accompanied by a gradual decrease in nuclear size, this upper peak might represent a fraction of neurons under transition between Inclusion– and Inclusion+ groups. The lack of a similar additional peak in the size distribution histogram for Inclusion+ group, however, does not support this interpretation. What is surprising is that this increase in nuclear size linked to NI formation (Inclusion+ group) was significant even when compared with the normal group. If NIs appeared in a certain phase during neurodegeneration usually characterized by reduction (atrophy) in cellular and nuclear size, it should have been observed in less atrophic nuclei rather than in hypertrophic ones. Even if this hypertrophic process represents an early phase of neurodegeneration before atrophy, its association with NIs implies that NI formation is linked, either directly or indirectly, to a mechanism that counteracts atrophy at least temporarily. Although an uneven shrinkage of a nucleus is potentially linked to its deformity, quantified as an increase in ratio and CI, this increase was not only restricted to Inclusion– group, but was also significant in Inclusion+ group with increased nuclear size. More evident indentation of the nuclear membrane has been observed even in normal neurons [21] and its pathological increase has been described in human brains with dentatorubral-pallidoluysian atrophy (DRPLA) [27], Huntington's disease (HD) [1] and its animal model [4]. Although our observation based on light microscopy failed to identify deep indentations of nuclear membrane, the increase in CI observed in NIID neurons either with or without NIs may represent another aspect of neurodegeneration, which is not necessarily linked to nuclear shrinkage.

Evidence and hypotheses are still conflicting on possible influence of NIs seen in brains with CAG/polyglutamine repeat disorders. Although both neurodegeneration and NI formation in transgenic models for HD are induced by a continued expression of the huntingtin fragment carrying expanded polyglutamine [35], or are suppressed by inhibition of caspase-1 [19], these two features are reportedly discrepant [10, 11, 20, 33] or even inversely related in cultured cells transfected with genes carrying expanded CAG repeat [22]. Similar discrepancy at tissue level has also been reported in human brains with HD [13]. This is also in agreement with our recent observation that cerebellar Purkinje cells of CAG/polyglutamine expansion disorders are more or less affected, but never exhibit NI [12]. The present work is the first morphometric study on human brains, which demonstrated an influence of NI of NIID on morphological aspects of each individual neuron with special attention to nucleus. Although it remains to be clarified how NI formation is related to neurodegeneration, suppression of NI formation by down-regulating ubiquitin-proteasome pathway has been reported to enhance cell death in vitro [3]. This mechanistic link between cell death and NI formation through ubiquitin-proteasome pathway implies that NI formation is inherently linked to a neuroprotective phenomenon mediated by ubiquitin. Our previous studies demonstrated that ubiquitin was localized to the periphery of NIs in both NIID [28] and SCA3 [6] brains. Similar organization of ubiquitin is also shared by another intranuclear inclusions, named Marinesco bodies, which arise in reaction to cellular stress, independently of expanded polyglutamine [7, 14]. Taken together, these findings are explained if NI formation mediated by ubiquitin is linked to a mechanism counteracting neuronal shrinkage in NIID, as reported in SCA1 [2]. Our recent morphometric study on brains with Machado-Joseph disease (MJD) demonstrated that nuclei of pontine neurons harboring NIs were larger than those not harboring NI [32]. A similar tendency was observed in cerebellar granule cells of DRPLA brains [27]. It is, therefore, very likely that such an influence of NI formation on nuclear size is shared among MJD, DRPLA and NIID. This implies that neurons are inherently equipped with machinery that counteracts shrinkage, triggered simultaneously during NI formation. It is essential to know whether this anti-atrophic influence of NI can be extrapolated to other disorders with ubiquitin-positive NIs in human brains. It is important to specify the molecular mechanism that regulates NI formation or neuronal degeneration together or separately. This will provide a rational background for reasonable treatment that may retard or even reverse neurodegeneration by activating or modulating this machinery.

Acknowledgements This work was supported in part by grants from Ministry of Health and Welfare (TH), from Human Science Foundation (TU) and from Japan Society for the Promotion of Science/INSERM (TU).

References

1. Bots GTAM, Bruyn GW (1981) Neuropathological changes of the nucleus accumbens in Huntington's chorea. Acta Neuropathol (Berl) 55:21–22
2. Cummings CJ, Mancini MA, Antalffy B, DeFranco DB, Orr HT, Zoghbi HY (1998) Chaperone suppression of aggregation and altered subcellular proteasome localization imply protein misfolding in SCA1. Nat Genet 19:148–154
3. Cummings CJ, Reinstein E, Sun Y, Antalffy B, Jiang Y-H, Ciechanover A, Orr HT, Beaudet AL, Zoghbi HY (1999) Mutation of the E6-AP ubiquitin ligase reduces nuclear inclusion frequency while accelerating polyglutamine-induced pathology in SCA1 mice. Cell 24:879–892

4. Davies SW, Turmaine M, Cozens BA, DiFiglia M, Sharp AH, Ross CA, Scherzinger E, Wanker EE, Mangiarini L, Bates GP (1997) Formation of neuronal intranuclear inclusions underlies the neurological dysfunction in mice transgenic for the HD mutation. Cell 90:537–548
5. Davies SW, Beardsall K, Turmaine M, DiFiglia M, Aronin N, Bates GP (1998) Are neuronal intranuclear inclusions the common neuropathology of triplet-repeat disorders with polyglutamine-repeat expansions? Lancet 351:131–133
6. Fujigasaki H, Uchihara T, Koyano S, Iwabuchi K, Yagishita S, Makifuchi T, Nakamura A, Ishida K, Toru S, Hirai S, Ishikawa K, Tanabe T, Mizusawa H (2000) Ataxin-3 is translocated into the nucleus for the formation of intranuclear inclusions in normal and Machado-Joseph disease brains. Exp Neurol 165:248–256
7. Fujigasaki H, Uchihara T, Takahashi J, Matsushita H, Nakamura A, Koyano S, Iwabuchi K, Hirai S, Mizusawa H (2001) Preferential recruitment of ataxin-3 independent of expanded polyglutamine: an immunohistochemical study on Marinesco bodies. J Neurol Neurosurg Psychiatry 71:518–520
8. Funata N, Maeda Y, Koike M, Yano Y, Kaseda M, Muro T, Okeda R, Iwata M, Yokoji M (1990) Neuronal intranuclear hyaline inclusion disease: report of a case and review of the literature. Clin Neuropathol 9:89–96
9. Hertwig R (1903) Über Korrelation von Zell- und Kerngrösse und ihre Bedeutung für die deschlechtliche Differenzierung und die Teilung der Zelle. Biol Zbl 23:49–119
10. Kim M, Lee H-S, LaForet G, McIntyre C, Matin EJ, Chang P, Kim TW, Williams M, Reddy PH, Tagle D, Boyce FM, Won L, Heller A, Aronin N, DiFiglia M (1999) Mutant huntingtin expression in clonal striatal cells: dissociation of inclusion formation and neuronal survival by caspase inhibition. J Neurochem 19:964–973
11. Klement IA, Skinner PJ, Kaytor MD, Yi H, Hersch SM, Clark HB, Zoghbi HY, Orr HT (1998) Ataxin-1 nuclear localization and aggregation: role in polyglutamine-induced disease in SCA1 transgenic mice. Cell 95:41–53
12. Koyano S, Iwabuchi K, Yagishita S, Kuroiwa Y, Uchihara T (2002) Paradoxical absence of nuclear inclusion in cerebellar Purkinje cells of hereditary ataxias linked to CAG expansion. J Neurol Neurosurg Psychiatry 73: 450–452
13. Kuemmerle S, Gutekunst C-A, Klein AM, Li X-J, Li S-H, Beal MF, Hersche SM, Ferrante RJ (1999) Huntingtin aggregates may not predict neuronal death in Huntington's disease. Ann Neurol 46:842–849
14. Kumada S, Uchihara T, Hayashi M, Nakamura A, Kikuchi E, Mizutani T, Oda M (in press) Promyelocytic leukemia protein is redistributed during the formation of intranuclear inclusions independent of polyglutamine expansion: an immunohistochemical study on Marinesco bodies. J Neuropathol Exp Neurol
15. Lieberman AP, Trojanowski JQ, Leonard DGB, Chen K-L, Bird TD, Robitaille Y, Malandrini A, Fischbeck KH (1999) Ataxin 1 and ataxin 3 in neuronal intranuclear inclusion disease. Ann Neurol 46:271–273
16. Malandrini A, Fabrizi MG, Cavallaro T, Berti G, Villanova M, Guazzi CG (1996) Neuronal intranuclear inclusion disease: polymerase chain reaction and ultrastructural study of rectal biopsy specimen in a new case. Acta Neuropathol 91:215–218
17. Montagne J (2000) Genetic and molecular mechanisms of cell size control. Mol Cell Biol Res Commun 4:195–202
18. Munoz-Garcia D, Ludwin SK (1986) Adult-onset neuronal intranuclear hyaline inclusion disease. Neurology 36:785–790
19. Ona VO, Li M, Vonsattel JP, Andrews LJ, Khan SQ, Chung WM, Frey AS, Menon AS, Li X-J, Stieg PE, Yuan J, Penney JB, Young AB, Cha J-HJ, Friedlander RM (1999) Inhibition of caspase-1 slows disease progression in a mouse model of Huntington's disease. Nature 399:263–267
20. Ordway JM, Tallaksen-Greene S, Gutekunst C-A, Bernstein EM, Cearley JA, Wiener HW, Dure IV LS, Lindsey R, Hersch SM, Jope RS, Albin RL, Detloff PJ (1997) Ectopically expressed CAG repeats cause intranuclear inclusions and a progressive late onset neurological phenotype in the mouse. Cell 91:753–763
21. Roos RAC, Bots GTAM (1983) Nuclear membrane indentations in Huntington's chorea. J Neurol Sci 61:37–47
22. Saudou F, Finkbeiner S, Devys D, Greenberg ME (1998) Huntingtin acts in the nucleus to induce apoptosis but death does not correlate with the formation of intranuclear inclusions. Cell 95: 55–66
23. Schuffler MD, Bird TD, Sumi SM, Cook A (1978) A familial neuronal disease presenting as intestinal pseudoobstruction. Gastroenterology 75:889–98
24. Sisodia SS (1998) Nuclear inclusions in glutamine repeat disorders: are they pernicious, coincidental, or beneficial? Cell 95: 1–4
25. Soffer D (1985) Neuronal intranuclear hyaline inclusion disease presenting as Friedreich's ataxia. Acta Neuropathol 65: 322–329
26. Sung JH, Ramirez-Lassepas M, Mastri AR, Larkin SM (1980) An unusual degenerative disorder of neurons associated with a novel intranuclear hyaline inclusion (neuronal intranuclear hyaline inclusion disease). A clinicopathological study of a case. J Neuropathol Exp Neurol 39:107–130
27. Takahashi H, Egawa S, Piao Y-S, Hayashi S, Yamada M, Oyanagi K, Tsuji S (2001) Neuronal nuclear alterations in dentatorubral-pallidoluysian atrophy: ultrastructural and morphometric studies of cerebellar granule cells. Brain Res 919:12–19
28. Takahashi J, Fukuda T, Tanaka J, Fujigasaki H, Minamitani, Uchihara T (2000) Neuronal intranuclear hyaline inclusion disease with polyglutamine immunoreactive inclusions. Acta Neuropathol 99:589–594
29. Takahashi J, Tanaka J, Arai K, Funata N, Hattori T, Fukuda T, Fujigasaki H, Uchihara T (2001) Recruitment of non-expanded polyglutamine proteins in intranuclear aggreages of neuronal intranuclear hyaline inclusion disease. J Neuropathol Exp Neurol 60:369–376
30. Tateishi J, Nagara H, Ohta M, Matsumoto T, Fukunaga H, Shida K (1984) Intranuclear inclusions in muscle, nervous tissue, and adrenal gland. Acta Neuropathol (Berl) 63:24–32
31. Uchihara T, Fujigasaki H, Koyano S, Nakamura A, Yagishita S, Iwabuchi K (2001) Non-expanded polyglutamine proteins in intranuclear inclusions of hereditary ataxias – triple-labeling immunofluorescence study. Acta Neuropathol 102:149–152
32. Uchihara T, Iwabuchi K, Funata N, Yagishita S (in press) Attenuated nuclear shrinkage in neurons with nuclear aggregates – a morphometric study on pontine neurons of Machado-Joseph disease brains. Exp Neurol
33. Watase K, Weeber EJ, Xu B, Antalffy B, Yuva-Paylor L, Hashimoto K, Kano M, Atkinson R, Sun Y, Armstrong DL, Sweatt JD, Orr HT, Paylor R, Zoghbi HY (2002) A long CAG repeat in the mouse sca1 locus replicates SCA1 features and reveals the impact of protein solubility on selective neurodegeneration. Neuron 34:905–919
34. Weidenheim KM, Dickson DW (1995) Intranuclear inclusion bodies in an elderly demented woman: a form of intranuclear inclusion body disease. Clin Neuropathol 14:93–99
35. Yamamoto A, Lucas JJ, Hen R (2000) Reversal of neuropathology and motor dysfunction in a conditional model of Huntington's disease. Cell 101:57–66
36. Zoghbi HY, Orr HT (2000) Glutamine repeats and neurodegeneration. Annu Rev Neurosci 2000:217–247

ELSEVIER

Journal of the Neurological Sciences 197 (2002) 79–84

Journal of the Neurological Sciences

www.elsevier.com/locate/jns

Short communication

Motor weakness and cerebellar ataxia in Sjögren syndrome—identification of antineuronal antibody: a case report

Kiyoshi Owada [a,b,*], Toshiki Uchihara [b,c], Kazuyuki Ishida [b,d], Hidehiro Mizusawa [b], Sadakiyo Watabiki [a], Kuniaki Tsuchiya [a,e]

[a] *Department of Neurology, Musashino Redcross Hospital, 1-26-1 Kyounan-cho, Musashino, Tokyo 180-8601, Japan*
[b] *Department of Neurology, Tokyo Medical and Dental University, Tokyo, Japan*
[c] *Department of Neuropathology, Tokyo Metropolitan Institute for Neuroscience, Tokyo, Japan*
[d] *Department of Neurology, Nissan Kousekai Tamagawa Hospital, Tokyo, Japan*
[e] *Department of Laboratory Medicine and Pathology, Tokyo Metropolitan Matsuzawa Hospital, Tokyo, Japan*

Received 3 January 2001; received in revised form 29 November 2001; accepted 5 February 2002

Abstract

We report here a combination of rare neurological manifestations of primary Sjögren syndrome (SS), such as motor-dominant motor weakness of peripheral origin, cerebellar ataxia and depression, in a Japanese female patient. An autoantibody in her serum and cerebrospinal fluid immunolabelled spinal motor neurons and cerebellar Purkinje cells. On Western blot, this antibody reacted with a protein of 34 kDa from the extract of spinal cord, dorsal root ganglion, or cerebellar cortex, which might correspond to motor weakness and cerebellar ataxia, respectively. The absence of its reactivity to the liver tissue indicates that this autoantibody targets an antigen represented exclusively in the neural tissues. Although it remains to be proved how autoantibodies, sometimes associated with SS, are involved in the development of clinical pictures, some of them are present in the cerebrospinal fluid and exhibit an exclusive affinity to neural tissues, which indicates its plausible link to neurological manifestations. Recognition of these antineuronal antibodies in SS will potentially provide a chance to treat these patients by removing or inactivating the antibody.

Keywords: Sjögren syndrome; Antineural antibody; Motor weakness; Cerebellar ataxia

1. Introduction

Primary Sjögren syndrome (SS) is a systematic autoimmune disorder characterized by keratoconjunctivitis and xerostomia. SS is known to accompany various kinds of neurological manifestations, most frequently, sensory-dominant peripheral neuropathy. Although the central nervous system is involved less frequently [1], psychiatric symptoms in SS have been also described [1–3]. Inflammatory cellular reactions into blood vessel (vasculitis) or dorsal root ganglion (ganglionitis) have been considered to represent a part of pathogenic processes leading to neurological manifestations of SS. On the other hand, humoral factor has recently been attracting increasing attention as one of the possible mediators of neurological manifestations [4–6]. We report here a Japanese female patient with SS, who manifested severe motor weakness, severe depressive state and cerebellar ataxia. In her serum and cerebrospinal fluid, we identified an autoantibody reacting with homogenized rat spinal cord, cerebrum, dorsal root ganglia (DRG) cerebellum. This autoantibody immunolabelled spinal motor neurons, cerebellar Purkinje cells and neurons in the cerebral cortex, which topographically corresponded to her neurological symptoms. The role of this autoantibody in the development of neurological symptoms will be discussed.

2. Case report

This 55-year-old Japanese female had been well until the age of 45 years, when she developed arthralgia in the extremities, low-grade fever and erythema, which subsided spontaneously. At age 50, she was admitted to a psychiatry

* Corresponding author. Present address: Department of Neurology, Tokyo Medical and Dental University, 1-5-45 Yushima, Bunkyo, Tokyo 113-8519, Japan. Tel.: +81-3-5803-5234; fax: +81-3-5803-0169.
E-mail address: 1730nuro@tmd.ac.jp (K. Owada).

0022-510X/02/$ - see front matter
PII: S0022-510X(02)00034-5